12
Weak Interactions

The observed lifetimes of the pion and muon are considerably longer than those of particles which decay either through color (i.e., strong) or electromagnetic interactions. It is found that

$$\begin{aligned} \pi^- &\to \mu^- \bar{\nu}_\mu \qquad \text{with } \tau = 2.6 \times 10^{-8} \text{ sec}, \\ \mu^- &\to e^- \bar{\nu}_e \nu_\mu \qquad \text{with } \tau = 2.2 \times 10^{-6} \text{ sec}, \end{aligned} \tag{12.1}$$

whereas particles decay by color interactions in about 10^{-23} sec and through electromagnetic interactions in about 10^{-16} sec (for example, $\pi^0 \to \gamma\gamma$). The lifetimes are inversely related to the coupling strength of these interactions, with the longer lifetime of the π^0 reflecting the fact that $\alpha \ll \alpha_s$. The pion and muon decays are evidence for another type of interaction with an even weaker coupling than electromagnetism.

Though all hadrons and leptons experience this weak interaction, and hence can undergo weak decays, they are often hidden by the much more rapid color or electromagnetic decays. However, the $\pi^\pm$ and μ are special. They cannot decay via the latter two interactions. The π is the lightest hadron. Whereas the neutral π can decay into photons, the charged pions cannot. As a result, the weak decay given in (12.1) is the dominant one. The reason why (12.1) is the dominant decay of the μ is interesting. In principle, the μ could decay electromagnetically via $\mu \to e\gamma$. The fact that the decay mode $\mu \to e\gamma$ is not seen and that the particular decay modes (12.1) occur are evidence for additive conserved lepton numbers: the electron number (L_e) and the muon number (L_μ). For example, the electron number assignments are

$$\begin{aligned} L_e &= +1: \quad e^- \text{ and } \nu_e, \\ L_e &= -1: \quad e^+ \text{ and } \bar{\nu}_e, \\ L_e &= 0: \quad \text{all other particles.} \end{aligned} \tag{12.2}$$

Similar assignments are made for L_μ and L_τ. Clearly, $L_\mu = 1$ and $L_e = 0$ for both the initial and final states of $\mu^- \to e^- \bar{\nu}_e \nu_\mu$, so this decay is consistent with the conservation of these quantum numbers; but $\mu^- \to e^- \gamma$ is not. In fact, known reactions conserve these three lepton numbers separately (see Section 12.12 for a further discussion).

EXERCISE 12.1 Give the π^+ and μ^+ decay processes. List the possible decay modes of the τ^- lepton (the τ is the third lepton in the sequence e, μ, τ with a mass $m_\tau = 1.8$ GeV).

The two examples of weak decays given in (12.1) involve neutrinos. Neutrinos are unique in that they can only interact by weak interactions. They are colorless and electrically neutral and, within experimental limits, also massless. Neutrinos are frequently found among the products of a weak decay, but not always. For example, a K^+ meson has the following weak decay modes:

$$\left.\begin{aligned} &K^+ \to \mu^+ \nu_\mu, e^+ \nu_e \\ &K^+ \to \pi^0 \mu^+ \nu_\mu, \pi^0 e^+ \nu_e \end{aligned}\right\} \quad \text{semileptonic decays,}$$
$$K^+ \to \pi^+ \pi^0, \pi^+ \pi^+ \pi^-, \pi^+ \pi^0 \pi^0 \quad \text{nonleptonic decays.} \tag{12.3}$$

The customary terminology is given on the right.

The weak interaction is also responsible for the β-decay of atomic nuclei, which involves the transformation of a proton to a neutron (or vice versa). Examples involving the emission of an $e^+ \nu_e$ lepton pair are

$$\begin{aligned} {}^{10}C &\to {}^{10}B^* + e^+ + \nu_e, \\ {}^{14}O &\to {}^{14}N^* + e^+ + \nu_e. \end{aligned} \tag{12.4}$$

Here, one of the protons in the nucleus transforms into a neutron via

$$p \to n e^+ \nu_e. \tag{12.5}$$

For free protons, this is energetically impossible (check the particle masses), but the crossed reaction, the β-decay process

$$n \to p e^- \bar{\nu}_e, \tag{12.6}$$

is allowed and is the reason for the neutron's instability (mean life 920 sec). Without the weak interaction, the neutron would be as stable as the proton, which has a lifetime in excess of 10^{30} years.

12.1 Parity Violation and the *V–A* Form of the Weak Current

Fermi's explanation of β-decay (1932) was inspired by the structure of the electromagnetic interaction. Recall that the invariant amplitude for electromagnetic electron–proton scattering (Fig. 12.1) is

$$\mathcal{M} = (e\bar{u}_p \gamma^\mu u_p)\left(\frac{-1}{q^2}\right)(-e\bar{u}_e \gamma_\mu u_e), \tag{12.7}$$

see (6.8), where we have treated the proton as a structureless Dirac particle. $\mathcal{M}$ is the product of the electron and proton electromagnetic currents, together with the propagator of the exchanged photon, see Section 6.2. To facilitate the comparison

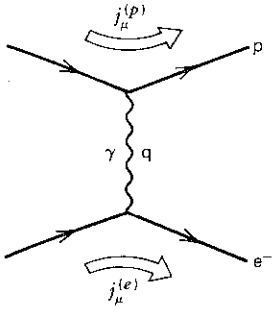

Fig. 12.1 Electron–proton (electromagnetic) scattering.

with weak interactions, we define, for example, an electron electromagnetic current of the form

$$ej_\mu^{em} \equiv j_\mu^{fi}(0) = -e\bar{u}_f\gamma_\mu u_i,$$

where $j_\mu^{fi}(x)$ is given by (6.6). Thus, the invariant amplitude, (12.7), becomes

$$\mathcal{M} = -\frac{e^2}{q^2}\left(j_\mu^{em}\right)_p\left(j^{em\mu}\right)_e.$$

The β-decay process (12.5), or its crossed form

$$\mathrm{pe}^- \rightarrow \mathrm{n}\nu_e,$$

is shown in Fig. 12.2. By analogy with the current–current form of (12.7), Fermi proposed that the invariant amplitude for β-decay be given by

$$\mathcal{M} = G\left(\bar{u}_n\gamma^\mu u_p\right)\left(\bar{u}_{\nu_e}\gamma_\mu u_e\right), \tag{12.8}$$

where G is the weak coupling constant which remains to be determined by experiment; G is called the Fermi constant. Note the charge-raising or charge-lowering structure of the weak current. We speak of these as the "charged weak currents." (The existence of a weak current that is electrically neutral, like the electromagnetic current, was not revealed until much later in 1973, see Section 12.9). Also note the absence of a propagator in (12.8). We return to this point in Section 12.2.

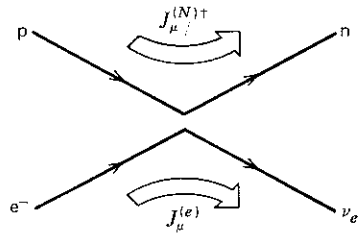

Fig. 12.2 The diagram for β-decay, $\mathrm{p} \rightarrow \mathrm{ne}^+\nu_e$, showing the weak currents.

Fermi's inspired guess of a vector–vector form of the weak amplitude $\mathfrak{M}$ is a very specific choice from among the various Lorentz invariant amplitudes that can in general be constructed using the bilinear covariants of (5.52). There is *a priori* no reason to use only vectors. The amplitude (12.8) explained the properties of some features of β-decay, but not others. Over the following 25 years or so, attempts to unravel the true form of the weak interaction led to a whole series of ingenious β-decay experiments, reaching a climax with the discovery of parity violation in 1956. Amazingly, the only essential change required in Fermi's original proposal was the replacement of γ^μ by $\gamma^\mu(1 - \gamma^5)$. Fermi had not foreseen parity violation and had no reason to include a $\gamma^5\gamma^\mu$ contribution; a mixture of γ^μ and $\gamma^5\gamma^\mu$ terms automatically violates parity conservation, see (5.67).

In 1956, Lee and Yang made a critical survey of all the weak interaction data. A particular concern at the time was the observed nonleptonic decay modes of the kaon, $K^+ \to 2\pi$ and 3π, in which the two final states have opposite parities. (People, in fact, believed that two different particles were needed to explain the two final states.) Lee and Yang argued persuasively that parity was not conserved in weak interactions. Experiments to check their assertion followed immediately. The first of these historic experiments serves as a good illustration of the effects of parity violation. The experiment studied β-transitions of polarized cobalt nuclei:

$$^{60}\mathrm{Co} \to {}^{60}\mathrm{Ni}^* + \mathrm{e}^- + \bar{\nu}_e.$$

The nuclear spins in a sample of ^{60}Co were aligned by an external magnetic field, and an asymmetry in the direction of the emitted electrons was observed. The asymmetry was found to change sign upon reversal of the magnetic field such that electrons prefer to be emitted in a direction opposite to that of the nuclear spin. The essence of the argument is sketched in Fig. 12.3. The observed correlation between the nuclear spin and the electron momentum is explained if the required $J_z = 1$ is formed by a right-handed antineutrino, $\bar{\nu}_R$, and a left-handed electron, e_L.

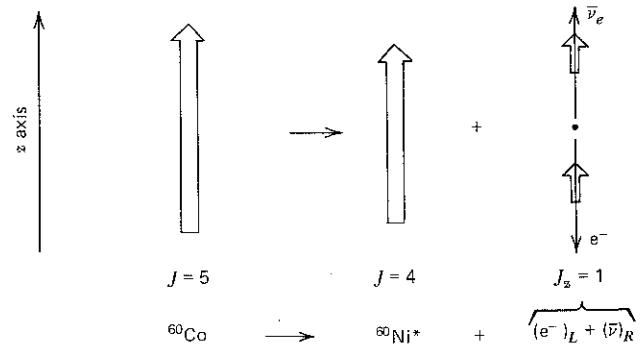

Fig. 12.3 The ^{60}Co experiment: the electron is emitted preferentially opposite the direction of the spin of the ^{60}Co nucleus.

The cumulative evidence of many experiments is that indeed only $\bar{\nu}_R$ (and ν_L) are involved in weak interactions. The absence of the "mirror image" states, $\bar{\nu}_L$ and ν_R, is a clear violation of parity invariance (see Section 5.7). Also, charge conjugation, C, invariance is violated, since C transforms a ν_L state into a $\bar{\nu}_L$ state. However, the $\gamma^\mu(1-\gamma^5)$ form leaves the weak interaction invariant under the combined CP operation. For instance,

$$\Gamma(\pi^+ \to \mu^+ \nu_L) \neq \Gamma(\pi^+ \to \mu^+ \nu_R) = 0 \qquad \text{P violation,}$$
$$\Gamma(\pi^+ \to \mu^+ \nu_L) \neq \Gamma(\pi^- \to \mu^- \bar{\nu}_L) = 0 \qquad \text{C violation,}$$

but

$$\Gamma(\pi^+ \to \mu^+ \nu_L) = \Gamma(\pi^- \to \mu^- \bar{\nu}_R) \qquad \text{CP invariance.}$$

In this example, ν denotes a muon neutrino. We discuss CP invariance in Section 12.13.

EXERCISE 12.2 Show that a (charge-lowering) weak current of the form

$$\bar{u}_e \gamma^\mu \tfrac{1}{2}(1-\gamma^5) u_\nu \tag{12.9}$$

involves only left-handed electrons (or right-handed positrons). In the relativistic limit ($v \approx c$), show that the electrons have negative helicity.

The $\frac{1}{2}(1-\gamma^5)$ in (12.9) automatically selects a left-handed neutrino (or a right-handed antineutrino). This V–A (vector–axial vector) structure of the weak current can be directly exposed by scattering ν_e's off electrons (see Section 12.7), just as the γ^μ structure of electromagnetism was verified by measurements of the angular distribution of e^+e^- scattering.

It is natural to hope that all weak interaction phenomena are described by a V–A current–current interaction with a universal coupling G. For example, β-decay of Fig. 12.2 and μ-decay of Fig. 12.4 can be described by the amplitudes

$$\mathcal{M}(p \to n e^+ \nu_e) = \frac{G}{\sqrt{2}} \left[\bar{u}_n \gamma^\mu (1-\gamma^5) u_p\right] \left[\bar{u}_{\nu_e} \gamma_\mu (1-\gamma^5) u_e\right] \tag{12.10}$$

and

$$\mathcal{M}(\mu^- \to e^- \bar{\nu}_e \nu_\mu) = \frac{G}{\sqrt{2}} \left[\bar{u}_{\nu_\mu} \gamma^\sigma (1-\gamma^5) u_\mu\right] \left[\bar{u}_e \gamma_\sigma (1-\gamma^5) u_{\nu_e}\right], \tag{12.11}$$

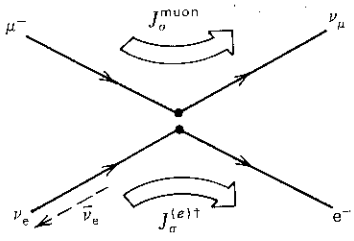

Fig. 12.4 The diagram for μ^- decay: $\mu^- \to e^- \bar{\nu}_e \nu_\mu$.

respectively. The $1/\sqrt{2}$ is pure convention (to keep the original definition of G which did not include γ^5). We then proceed in analogy with the Feynman rules for QED. The calculations only involve particles, and the diagrams show only particle lines. Antiparticles do not appear. Thus, the outgoing $\bar{\nu}_e$ (of momentum k) in μ-decay is shown in Fig. 12.4 as an ingoing ν_e (of momentum $-k$). As before, the spinor $u_{\nu_e}(-k)$ of (12.11) will be denoted $v_{\nu_e}(k)$, see (5.33). The same remarks apply to the outgoing e^+ of (12.10).

EXERCISE 12.3 Show that the *charge-raising* weak current

$$J^\mu = \bar{u}_\nu \gamma^\mu \tfrac{1}{2}(1 - \gamma^5) u_e \tag{12.12}$$

couples an ingoing negative helicity electron to an outgoing negative helicity neutrino. Neglect the mass of the electron. Besides the configuration (e_L^-, ν_L), show that J^μ also couples the following (ingoing, outgoing) lepton pair configurations: $(\bar{\nu}_R, e_R^+)$, $(0, \nu_L e_R^+)$, and $(e_L^- \bar{\nu}_R, 0)$.

Further, show that the *charge-lowering* weak current, (12.9), is the hermitian conjugate of (12.12):

$$J_\mu^\dagger = \bar{u}_e \gamma_\mu \tfrac{1}{2}(1 - \gamma^5) u_\nu.$$

List the lepton pair configurations coupled by $J_\mu^\dagger$.

Weak interaction amplitudes are of the form

$$\boxed{\mathcal{M} = \frac{4G}{\sqrt{2}} J^\mu J_\mu^\dagger.} \tag{12.13}$$

Charge conservation requires that $\mathcal{M}$ is the product of a charge-raising and a charge-lowering current; see, for example, (12.10) and (12.11). The factor 4 arises because the currents, (12.13), are defined with the normalized projection operator $\frac{1}{2}(1 - \gamma^5)$ rather than the old-fashioned $(1 - \gamma^5)$.

12.2 Interpretation of the Coupling G

We can use the observed rates for nuclear β-decay and for μ-decay to obtain a numerical value for G. It is also crucial to check the universality of the strength of the weak coupling constant G of (12.10) and (12.11). We do not want to introduce a new interaction for every weak process! However, because we do this, let us cast G in a form that can be directly compared to the couplings of the color and electromagnetic interactions.

Examination of the electromagnetic and the weak amplitudes of (12.7) and (12.10) shows that in Fermi's model the analogy between the two interactions has not been fully developed. We see that G essentially replaces e^2/q^2. Thus, G, in

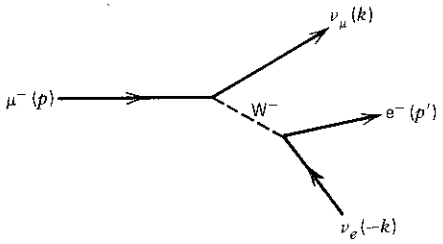

Fig. 12.5 Muon decay.

contrast to the dimensionless coupling e, has dimensions GeV^{-2}. It is tempting to try and extend the analogy by postulating that the weak interactions are generated by the emission and absorption of charged vector bosons, which we call weak bosons, $W^{\pm}$. The weak bosons are the analogues of the photon for the electromagnetic force and the gluons for the color force. For example, μ^- decay is mediated by a W^- boson (see Fig. 12.5) and the amplitude is of the form [see (12.7)]

$$\mathcal{M} = \left(\frac{g}{\sqrt{2}}\bar{u}_{\nu_\mu}\gamma^\sigma\tfrac{1}{2}(1-\gamma^5)u_\mu\right)\frac{1}{M_W^2 - q^2}\left(\frac{g}{\sqrt{2}}\bar{u}_e\gamma_\sigma\tfrac{1}{2}(1-\gamma^5)u_{\nu_e}\right), \tag{12.14}$$

where $g/\sqrt{2}$ is a dimensionless weak coupling and q is the momentum carried by the weak boson (the factors $1/\sqrt{2}$ and $\frac{1}{2}$ are inserted so that we have the conventional definition of g). In contrast to the photon, the weak boson must be massive, otherwise it would have been directly produced in weak decays. Indeed, it turns out that $M_W \sim 80$ GeV (see Chapter 15).

In (12.14), we have been cavalier about the spin sum in the boson propagator, see (6.87). However, at the moment, we are interested in situations where $q^2 \ll M_W^2$ (e.g., β-decay and μ-decay). Then, (12.14) reverts to (12.11) with

$$\frac{G}{\sqrt{2}} = \frac{g^2}{8M_W^2} \tag{12.15}$$

and the weak currents interact essentially at a point. That is, in the limit (12.15), the propagator between the currents disappears. Equation (12.15) prompts the idea that weak interactions are weak not because $g \ll e$, but because M_W^2 is large. If indeed $g \approx e$, then at energies $O(M_W)$ and above, the weak interaction would become of comparable strength to the electromagnetic interaction.

We may think of $g \approx e$ as a unification of weak and electromagnetic interactions in much the same way as the unification of the electric and magnetic forces in Maxwell's theory of electromagnetism, where

$$\mathbf{F} = e\mathbf{E} + e_M\mathbf{v} \times \mathbf{B}$$

with $e_M = e$. At low velocities, the magnetic forces are very weak, whereas for high-velocity particles, the electric and magnetic forces play a comparable role.

The velocity of light c is the scale which governs the relative strength. The analogue for the electroweak force is M_W on the energy scale. The unification of the electromagnetic and weak forces is the subject of Chapters 13 and 15.

12.3 Nuclear β-Decay

Let us use the observed transition rate of the process

$$^{14}\mathrm{O} \rightarrow {}^{14}\mathrm{N}^* + \mathrm{e}^+ + \nu_e$$

to estimate G. By analogy with the QED calculations of Section 6.2, we write the transition amplitude for this process (Fig. 12.2) in the form

$$T_{fi} = -i\frac{4G}{\sqrt{2}}\int J_\mu^{(N)\dagger}(x)\,J^{(e)\mu}(x)\,d^4x \tag{12.16}$$

$$= -i\frac{4G}{\sqrt{2}}\int\left[\bar{\psi}_n(x)\gamma_\mu\tfrac{1}{2}(1-\gamma^5)\psi_p(x)\right]\left[\bar{\psi}_\nu(x)\gamma^\mu\tfrac{1}{2}(1-\gamma^5)\psi_e(x)\right]d^4x, \tag{12.17}$$

see (12.10). For this problem, it is easier not to perform the x integration at this stage. Remember that usually we carry out the x integration and obtain $(2\pi)^4$ times the "energy–momentum conserving" delta function (see Section 6.2). We then define

$$T_{fi} = -i(2\pi)^4\,\delta^{(4)}(p_p - p_n - p_e - p_\nu)\,\mathfrak{M}.$$

Thus, (12.16) reduces to the form (12.13).

In writing down (12.16), we have assumed that the other nucleons in ^{14}O are simply spectators to the decaying proton. However, *a priori*, we cannot ignore the fact the nucleons participating in β-decay are bound inside nuclei. We also have no reason to believe the idealized form of weak nucleon current, $J^{(N)}$, shown in (12.17), since the nucleons themselves are composite objects and not structureless Dirac particles. Despite these problems, it turns out to be quite easy to get an accurate estimate of G. There are several reasons for this. First, the low-energy weak interaction is essentially a point interaction, and we can ignore the longer-range strong interaction effects we just mentioned. Actually, there is a beautiful and more precise justification for this vague argument. The weak current $(\bar{\psi}_p\gamma^\mu\psi_n)$ and its conjugate $(\bar{\psi}_n\gamma^\mu\psi_p)$, together with the electromagnetic current $(\bar{\psi}_p\gamma^\mu\psi_p)$, are believed to form an isospin triplet of conserved vector currents. This is referred to as the *conserved vector current hypothesis*. The intimate connection with the electromagnetic current "protects" the vector part of the weak current from any strong interaction corrections, just as the electromagnetic charge is protected. The axial vector part, $\bar{\psi}_n\gamma^\mu\gamma^5\gamma_p$, will not contribute to the process as we are considering a transition between two $J^P = 0^+$ nuclear states,

which precludes a change of parity. Moreover, since the process occurs between two $J = 0$ nuclei, we can safely assume that the nuclear wavefunction is essentially unchanged by the transition.

Another simplifying feature is that the energy released in the decay (about 2 MeV) is small compared to the rest energy of the nuclei. We can therefore use nonrelativistic spinors for the nucleons [see (6.11)], and then only γ^μ with $\mu = 0$ contributes [see (6.13)]. Thus,

$$T_{fi} \simeq -i\frac{G}{\sqrt{2}}\left[\bar{u}(p_\nu)\gamma^0(1-\gamma^5)v(p_e)\right]\int\psi_n^\dagger(x)\psi_p(x)e^{-i(p_\nu+p_e)\cdot x}\,d^4x, \tag{12.18}$$

where, as remarked after (12.11), the v spinor $v(p_e)$ describes an outgoing positron of momentum p_e. The e^+ and ν are emitted with an energy of the order of 1 MeV, and so their de Broglie wavelengths are about 10^{-11} cm, which is much larger than the nuclear diameter. We can therefore set

$$e^{i(\mathbf{p}_\nu+\mathbf{p}_e)\cdot\mathbf{x}} \simeq 1$$

and perform the spatial integration of (12.18). Noting the relation between T_{fi} and the invariant amplitude $\mathfrak{M}$ (see Section 6.2), we obtain

$$\mathfrak{M} = \frac{G}{\sqrt{2}}\left(\bar{u}(p_\nu)\gamma^0(1-\gamma^5)v(p_e)\right)(2m_N)\left(2\sqrt{\tfrac{1}{2}}\right), \tag{12.19}$$

where $2m_N$ arises from the normalization of the nucleon spinors [see (6.13)] and $2/\sqrt{2}$ is the hadronic isospin factor for the $^{14}\mathrm{O} \to {}^{14}\mathrm{N}^*$ transition (see Exercise 12.4).

EXERCISE 12.4 Verify the isospin factor $\sqrt{2}$ in (12.19). Note that ^{14}C, ^{14}N*, ^{14}O form an isospin triplet, which can be viewed as nn, np, pp, together with an isospin zero ^{12}C core (see Fig. 2.2). Keep in mind that for indistinguishable proton decays, we must add amplitudes, not probabilities.

The rate $d\Gamma$ for the "p" $\to$ "n"$e^+\nu$ transition is related to $|\mathfrak{M}|^2$ by (4.36). We obtain

$$d\Gamma = G^2\sum_{\text{spins}}\left|\bar{u}(p_\nu)\gamma^0(1-\gamma^5)v(p_e)\right|^2\frac{d^3p_e}{(2\pi)^3 2E_e}$$
$$\times\frac{d^3p_\nu}{(2\pi)^3 2E_\nu}2\pi\,\delta(E_0-E_e-E_\nu), \tag{12.20}$$

where E_0 is the energy released to the lepton pair. The normalization factor $(2m_N)^2$ cancels with the equivalent $2E_p\,2E_n$ factor in (4.36), as indeed it must. The summation over spins can be performed using the techniques we introduced

in Chapter 6. Neglecting the mass of the electron, we have

$$\begin{aligned}\sum_{\text{spins}} \left|\bar{u}\gamma^0(1-\gamma^5)v\right|^2 &= \sum \left(\bar{u}\gamma^0(1-\gamma^5)v\right)\left(\bar{v}(1+\gamma^5)\gamma^0 u\right) \\ &= \mathrm{Tr}\left(\not{p}_\nu\gamma^0(1-\gamma^5)\not{p}_e(1+\gamma^5)\gamma^0\right) \\ &= 2\mathrm{Tr}\left(\not{p}_\nu\gamma^0\not{p}_e(1+\gamma^5)\gamma^0\right) \\ &= 8(E_eE_\nu + \mathbf{p}_e\cdot\mathbf{p}_\nu) \\ &= 8E_eE_\nu(1+v_e\cos\theta), \end{aligned} \tag{12.21}$$

where θ is the opening angle between the two leptons and where the electron velocity $v_e \simeq 1$ in our approximation. Here, we have used the trace theorems of Section 6.4; see also (12.25) and (12.26). Substituting (12.21) into (12.20), the transition rate becomes

$$d\Gamma = \frac{2G^2}{(2\pi)^5}(1+\cos\theta)\left[(2\pi d\cos\theta p_e^2\, dp_e)(4\pi E_\nu^2 dE_\nu)\right]\delta(E_0 - E_e - E_\nu), \tag{12.22}$$

where $d^3p_e\, d^3p_\nu$ has been replaced by the expression in the square brackets.

Many experiments focus attention on the energy spectrum of the emitted positron. From (12.22), we obtain

$$\begin{aligned}\frac{d\Gamma}{dp_e} &= \frac{4G^2}{(2\pi)^3}p_e^2(E_0-E_e)^2\int d\cos\theta(1+\cos\theta) \\ &= \frac{G^2}{\pi^3}p_e^2(E_0-E_e)^2. \end{aligned} \tag{12.23}$$

Thus, if from the observed positron spectrum we plot $p_e^{-1}(d\Gamma/dp_e)^{1/2}$ as a function of E_e, we should obtain a linear plot with end point E_0. This is called the Kurie plot. It can be used to check whether the neutrino mass is indeed zero. A nonvanishing neutrino mass destroys the linear behavior, particularly for E_e near E_0. (In practice, of course, we must examine the approximations we have made, correct E_e for the energy gained from the nuclear Coulomb field, and allow for the experimental energy resolution.)

Our immediate interest here is of a different nature. We wish to determine G from the observed value E_0 and the measured lifetime τ of the nuclear state to β-decay. We therefore carry out the dp_e integration of (12.23) over the interval 0, E_0. Making the relativistic approximation $p_e \approx E_e$, we find

$$\boxed{\Gamma = \frac{1}{\tau} = \frac{G^2E_0^5}{30\pi^3}.}$$

Now, for $^{14}\mathrm{O} \rightarrow {}^{14}\mathrm{N}^*\mathrm{e}^+\nu$, the nuclear energy difference E_0 is 1.81 MeV, and

the measured half-life is $\tau \log 2 = 71$ sec. Using this information, we find

$$G \simeq 10^{-5}/m_N^2. \tag{12.24}$$

Recall that G has dimension (mass)$^{-2}$. We have chosen to quote the value with respect to the nucleon mass.

EXERCISE 12.5 Calculate G from the data for the β-transition $^{10}\mathrm{C} \to {}^{10}\mathrm{B}^*\mathrm{e}^+\nu$. The measured half-life is $\tau \log 2 = 20$ sec, and $E_0 = 2$ MeV. (^{10}C and ^{10}B* are both isospin 1, $J^P = 0^+$ states.)

EXERCISE 12.6 Accepting the vector boson exchange picture of weak interactions with coupling, $g = e$, estimate the mass M_W of the weak boson. (In the standard model of weak interactions, introduced in Chapter 13, $g \sin\theta_W = e$, with $\sin^2\theta_W \approx \frac{1}{4}$.)

12.4 Further Trace Theorems

We collect together some results that are useful for the computation of weak interaction processes and that follow directly from the trace theorems of Section 6.4:

$$\mathrm{Tr}(\gamma^\mu \not{p}_1 \gamma^\nu \not{p}_2) = 4\left[p_1^\mu p_2^\nu + p_1^\nu p_2^\mu - (p_1 \cdot p_2) g^{\mu\nu}\right], \tag{12.25}$$

$$\mathrm{Tr}\left[\gamma^\mu(1-\gamma^5)\not{p}_1\gamma^\nu(1-\gamma^5)\not{p}_2\right] = 2\mathrm{Tr}(\gamma^\mu \not{p}_1 \gamma^\nu \not{p}_2) + 8i\varepsilon^{\mu\alpha\nu\beta} p_{1\alpha} p_{2\beta}, \tag{12.26}$$

$$\begin{aligned}&\mathrm{Tr}(\gamma^\mu \not{p}_1 \gamma^\nu \not{p}_2)\,\mathrm{Tr}(\gamma_\mu \not{p}_3 \gamma_\nu \not{p}_4)\\ &\quad = 32\left[(p_1 \cdot p_3)(p_2 \cdot p_4) + (p_1 \cdot p_4)(p_2 \cdot p_3)\right],\end{aligned} \tag{12.27}$$

$$\begin{aligned}&\mathrm{Tr}(\gamma^\mu \not{p}_1 \gamma^\nu \gamma^5 \not{p}_2)\,\mathrm{Tr}(\gamma_\mu \not{p}_3 \gamma_\nu \gamma^5 \not{p}_4)\\ &\quad = 32\left[(p_1 \cdot p_3)(p_2 \cdot p_4) - (p_1 \cdot p_4)(p_2 \cdot p_3)\right],\end{aligned} \tag{12.28}$$

$$\begin{aligned}&\mathrm{Tr}\left[\gamma^\mu(1-\gamma^5)\not{p}_1\gamma^\nu(1-\gamma^5)\not{p}_2\right]\mathrm{Tr}\left[\gamma_\mu(1-\gamma^5)\not{p}_3\gamma_\nu(1-\gamma^5)\not{p}_4\right]\\ &\quad = 256(p_1 \cdot p_3)(p_2 \cdot p_4).\end{aligned} \tag{12.29}$$

EXERCISE 12.7 Verify these results.

12.5 Muon Decay

Muon decay,

$$\mu^-(p) \to \mathrm{e}^-(p') + \bar{\nu}_e(k') + \nu_\mu(k), \tag{12.30}$$

is the model reaction for weak decays. The particle four-momenta are defined in (12.30), and the Feynman diagram is shown in Fig. 12.5. According to the Feynman rules, it must be drawn using only particle lines; and so the outgoing $\bar{\nu}_e$ is shown as an incoming ν_e. The invariant amplitude for muon decay is

$$\mathfrak{M} = \frac{G}{\sqrt{2}}\left[\bar{u}(k)\gamma^\mu(1-\gamma^5)u(p)\right]\left[\bar{u}(p')\gamma_\mu(1-\gamma^5)v(k')\right], \tag{12.31}$$

see (12.11), where the spinors are labeled by the particle momenta. Recall that the outgoing $\bar{\nu}_e$ is described by $v(k')$. The muon decay rate can now be obtained using (4.36),

$$d\Gamma = \frac{1}{2E}\overline{|\mathcal{M}|^2}dQ \tag{12.32}$$

where the invariant phase space is

$$\begin{aligned} dQ &= \frac{d^3p'}{(2\pi)^3 2E'}\frac{d^3k}{(2\pi)^3 2\omega}\frac{d^3k'}{(2\pi)^3 2\omega'}(2\pi)^4\delta^{(4)}(p-p'-k-k') \\ &= \frac{1}{(2\pi)^5}\frac{d^3p'}{2E'}\frac{d^3k'}{2\omega'}\theta(E-E'-\omega')\delta\big((p-p'-k')^2\big), \end{aligned} \tag{12.33}$$

with $p^0 \equiv E$, $k^0 \equiv \omega$, and so on, and where in reaching the last line we have performed the d^3k integration using

$$\int \frac{d^3k}{2\omega} = \int d^4k\,\theta(\omega)\delta(k^2). \tag{12.34}$$

EXERCISE 12.8 Derive (12.34) by performing the $d\omega$ integration on the right-hand side (see Exercise 6.7).

Using (12.31) and (12.29), we find the spin-averaged probability is

$$\overline{|\mathcal{M}|^2} \equiv \frac{1}{2}\sum_{\text{spins}}|\mathcal{M}|^2 = 64G^2(k\cdot p')(k'\cdot p), \tag{12.35}$$

where $p = p' + k + k'$ on account of the d^4k integration performed in (12.33). Since $m_\mu > 200m_e$, we can safely neglect the mass of the electron.

EXERCISE 12.9 Verify (12.35). Neglect the mass of the electron, but not that of the muon.

EXERCISE 12.10 Show that

$$2(k\cdot p')(k'\cdot p) = (p-k')^2(k'\cdot p) = (m^2 - 2m\omega')m\omega' \tag{12.36}$$

in the muon rest frame, where $p = (m, 0, 0, 0)$.

Gathering these results together, the decay rate in the muon rest frame is

$$\begin{aligned} d\Gamma = \frac{G^2}{2m\pi^5}\frac{d^3p'}{2E'}\frac{d^3k'}{2\omega'}&m\omega'(m^2-2m\omega') \\ &\times\delta(m^2 - 2mE' - 2m\omega' + 2E'\omega'(1-\cos\theta)), \end{aligned} \tag{12.37}$$

and, as for β-decay, we can replace $d^3p'\,d^3k'$ by

$$4\pi E'^2\,dE'\,2\pi\omega'^2\,d\omega' d\cos\theta.$$

We now use the fact that

$$\delta(\cdots + 2E'\omega'\cos\theta) = \frac{1}{2E'\omega'}\delta(\cdots - \cos\theta)$$

to perform the integration over the opening angle θ between the emitted e^- and $\bar{\nu}_e$ and obtain

$$d\Gamma = \frac{G^2}{2\pi^3}dE'\,d\omega'\,m\omega'(m - 2\omega'). \tag{12.38}$$

The δ-function integration introduces the following restrictions on the energies E', ω', stemming from the fact that $-1 \le \cos\theta \le 1$:

$$\tfrac{1}{2}m - E' \le \omega' \le \tfrac{1}{2}m, \tag{12.39}$$

$$0 \le E' \le \tfrac{1}{2}m. \tag{12.40}$$

These limits are easily understood in terms of the various limits in which the three-body decay $\mu \to e\bar{\nu}_e\nu_\mu$ becomes effectively a two-body decay. For example, when the electron energy E' vanishes, (12.39) yields $\omega' = m/2$, which is expected because then the two neutrinos share equally the muon's rest energy.

To obtain the energy spectrum of the emitted electron, we perform the ω' integration of (12.38):

$$\frac{d\Gamma}{dE'} = \frac{mG^2}{2\pi^3}\int_{\frac{1}{2}m-E'}^{\frac{1}{2}m} d\omega'\,\omega'(m - 2\omega')$$

$$= \frac{G^2}{12\pi^3}m^2E'^2\left(3 - \frac{4E'}{m}\right). \tag{12.41}$$

This prediction is in excellent agreement with the observed electron spectrum. Finally, we calculate the muon decay rate

$$\boxed{\Gamma \equiv \frac{1}{\tau} = \int_0^{m/2} dE'\,\frac{d\Gamma}{dE'} = \frac{G^2m^5}{192\pi^3}.} \tag{12.42}$$

Inserting the measured muon lifetime $\tau = 2.2 \times 10^{-6}$ sec, we can calculate the Fermi coupling G. We find

$$G \sim 10^{-5}/m_N^2. \tag{12.43}$$

Comparison of the values of G obtained in (12.24) and (12.43) supports the assertion that the weak coupling constant is the same for leptons and nucleons, and hence universal. It means that nuclear β-decay and the decay of the muon have the same physical origin. Indeed, when all corrections are taken into

account, G_β and G_μ are found to be equal to within a few percent:

$$G_\mu = (1.16632 \pm 0.00002) \times 10^{-5}\ \text{GeV}^{-2},$$
$$G_\beta = (1.136 \pm 0.003) \times 10^{-5}\ \text{GeV}^{-2}. \tag{12.44}$$

The reason for the small difference is important and is discussed in Section 12.11 [see (12.107)].

EXERCISE 12.11 Draw a diagram showing the particle helicities in the μ^- rest frame in the case where the emitted electron has its maximum permissible energy. In this limit, explain why the electron angular distribution has the form $1 - P\cos\alpha$, where **P** is the polarization of the muon and α is the angle between the polarization direction and the direction of the emitted electron:

$$P \equiv \frac{N_+ - N_-}{N_+ + N_-},$$

where $N_\pm$ are the numbers of spin-up, spin-down muons.

EXERCISE 12.12 "Predict" the rate for the decay $\tau^- \to e^- \bar{\nu}_e \nu_\tau$, where the τ-lepton has mass 1.8 GeV. The observed branching ratio of this decay mode is approximately 20%. Calculate the lifetime of the τ-lepton. Can you explain this branching ratio?

12.6 Pion Decay

Can we now also understand the lifetime of the $\pi^\pm$-mesons? To be specific, we take the decay

$$\pi^-(q) \to \mu^-(p) + \bar{\nu}_\mu(k), \tag{12.45}$$

which is shown in Fig. 12.6. The amplitude is of the form

$$\mathcal{M} = \frac{G}{\sqrt{2}}(\ldots)^\mu \bar{u}(p)\gamma_\mu(1 - \gamma^5)v(k) \tag{12.46}$$

where $(\ldots)$ represents the weak quark current of Fig. 12.6. It is tempting to write it as $\bar{u}_d\gamma^\mu(1 - \gamma^5)v_{\bar{u}}$, but this is incorrect since the $\bar{u}$, d quarks in Fig. 12.6 are not free quark states but are quarks bound into a π^--meson. We know, however, that

- $\mathcal{M}$ is Lorentz invariant, so that $(\ldots)^\mu$ must be a vector or axial-vector, as indicated.
- The π^- is spinless, so that q is the only four-vector available to construct $(\ldots)^\mu$.

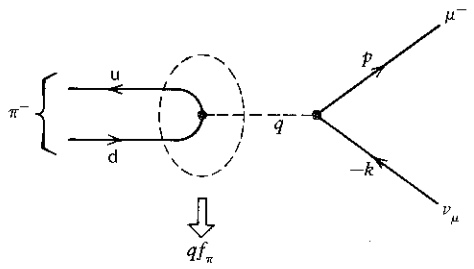

Fig. 12.6 Feynman diagram for the decay $\pi^-(\bar{u}d) \to \mu^-\bar{\nu}_\mu$ with four-momentum $q = p + k$.

We therefore have

$$(\ldots)^\mu = q^\mu f(q^2) \equiv q^\mu f_\pi, \tag{12.47}$$

where f is a function of q^2 since it is the only Lorentz scalar that can be formed from q, but $q^2 = m_\pi^2$ and $f(m_\pi^2) \equiv f_\pi$ is a constant. Inserting (12.47) into (12.46), the $\pi^- \to \mu^-\bar{\nu}$ decay amplitude is

$$\begin{aligned}\mathcal{M} &= \frac{G}{\sqrt{2}}(p^\mu + k^\mu) f_\pi \left[\bar{u}(p)\gamma_\mu(1-\gamma^5)v(k)\right] \\ &= \frac{G}{\sqrt{2}} f_\pi m_\mu \bar{u}(p)(1-\gamma^5)v(k).\end{aligned} \tag{12.48}$$

Here, we have used $\not{k}v(k) = 0$ and $\bar{u}(p)(\not{p} - m_\mu) = 0$, the Dirac equations for the neutrino and muon, respectively. In its rest frame, the π-decay rate is

$$d\Gamma = \frac{1}{2m_\pi}\overline{|\mathcal{M}|^2}\frac{d^3p}{(2\pi)^3 2E}\frac{d^3k}{(2\pi)^3 2\omega}(2\pi)^4\,\delta(q-p-k), \tag{12.49}$$

where the sum over the spins of the outgoing lepton pair can be performed by familiar traceology [see (6.22) and (6.23)]:

$$\begin{aligned}\overline{|\mathcal{M}|^2} &= \frac{G^2}{2} f_\pi^2 m_\mu^2 \mathrm{Tr}\left((\not{p} + m_\mu)(1-\gamma^5)\not{k}(1+\gamma^5)\right) \\ &= 4G^2 f_\pi^2 m_\mu^2 (p\cdot k).\end{aligned} \tag{12.50}$$

In the π rest frame ($\mathbf{k} = -\mathbf{p}$),

$$p\cdot k = E\omega - \mathbf{k}\cdot\mathbf{p} = E\omega + \mathbf{k}^2 = \omega(E+\omega). \tag{12.51}$$

Gathering these results together, we have

$$\Gamma = \frac{G^2 f_\pi^2 m_\mu^2}{(2\pi)^2 2m_\pi}\int \frac{d^3p\,d^3k}{E\omega}\delta(m_\pi - E - \omega)\,\delta^{(3)}(\mathbf{k}+\mathbf{p})\,\omega(E+\omega).$$

The d^3p integration is taken care of by the $\delta^{(3)}$ function and, since there is no angular dependence, we are left with only the integration over $d\omega$:

$$\Gamma = \frac{G^2 f_\pi^2 m_\mu^2}{(2\pi)^2 2m_\pi} 4\pi \int d\omega\, \omega^2 \left(1 + \frac{\omega}{E}\right) \delta(m_\pi - E - \omega), \tag{12.52}$$

where $E = (m_\mu^2 + \omega^2)^{1/2}$. The result of the integration is ω_0^2, where

$$\omega_0 \equiv \frac{m_\pi^2 - m_\mu^2}{2m_\pi}. \tag{12.53}$$

This can be seen by rewriting the δ-function in (12.52) as

$$\delta[f(\omega)] = \delta(\omega - \omega_0) \Big/ \left|\frac{\partial f}{\partial \omega}\right|_{\omega=\omega_0} = \delta(\omega - \omega_0) \Big/ \left(1 + \frac{\omega_0}{E}\right).$$

Therefore, finally we obtain

$$\boxed{\Gamma = \frac{1}{\tau} = \frac{G^2}{8\pi} f_\pi^2 m_\pi m_\mu^2 \left(1 - \frac{m_\mu^2}{m_\pi^2}\right)^2}. \tag{12.54}$$

Taking the universal value of $G = 10^{-5}\, m_N^{-2}$ obtained from β- or μ-decay and assuming that $f_\pi = m_\pi$ (a guess which at least guarantees the correct dimension), we indeed obtain the π^- lifetime announced at the beginning of the chapter. Although the theory can clearly accommodate the long lifetime of the charged π, the decay does not provide a quantitative test, as $f_\pi = m_\pi$ is a pure guess.

A quantitative test, however, is possible. If we repeat the calculation for the decay mode $\pi^- \to e^- \bar{\nu}_e$, we obtain (12.54) with m_μ replaced by m_e. Therefore,

$$\frac{\Gamma(\pi^- \to e^- \bar{\nu}_e)}{\Gamma(\pi^- \to \mu^- \bar{\nu}_\mu)} = \left(\frac{m_e}{m_\mu}\right)^2 \left(\frac{m_\pi^2 - m_e^2}{m_\pi^2 - m_\mu^2}\right)^2 = 1.2 \times 10^{-4}, \tag{12.55}$$

where the numerical value comes from inserting the particle masses. The charged π prefers (by a factor of 10^4) to decay into a muon, which has a similar mass, rather than into the much lighter electron. This is quite contrary to what one would expect from phase–space considerations, so some dynamical mechanism must be at work.

The pion is spinless, and so, by the conservation of angular momentum, the outgoing lepton pair ($e^- \bar{\nu}_e$) must have $J = 0$. As the $\bar{\nu}_e$ has positive helicity, the e^- is also forced into a positive helicity state, see Fig. 12.7. But recall that this is

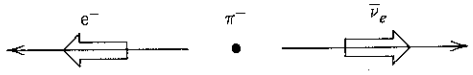

Fig. 12.7 The decay $\pi^- \to e^- \bar{\nu}_e$ showing the right-handed helicity of the outgoing leptons.

the "wrong" helicity state for the electron. In the limit $m_e = 0$, the weak current only couples negative helicity electrons, and hence the positive helicity coupling is highly suppressed. Thus, in the π^--decay, the e^- (or μ^-) is forced by angular momentum conservation into its "wrong" helicity state. This is much more likely to happen for the μ^- than for the relatively light e^-, in fact, 10^4 times more likely. Experiment confirms this result, which is a direct consequence of the $1 - \gamma^5$ or left-handed structure of the weak current, (12.12). It is however interesting to note that prior to the discovery of parity violation, an argument for (12.55) based on helicity conservation was proposed by Ruderman and Finkelstein (1949) (*Phys. Rev.* **76**, 1458).

EXERCISE 12.13 Predict the ratio of the $K^- \to e^- \bar{\nu}_e$ and $K^- \to \mu^- \bar{\nu}_\mu$ decay rates. Given that the lifetime of the K^- is $\tau = 1.2 \times 10^{-8}$ sec and the $K \to \mu\nu$ branching ratio is 64%, estimate the decay constant f_K. Comment on your assumptions and on your result.

12.7 Charged Current Neutrino–Electron Scattering

Although the experiments exposing the violation of parity in weak interactions (polarized ^{60}Co decay, K decay, π-decay, etc.) are some of the highlights in the development of particle physics, parity violation and its V–A structure can now be demonstrated experimentally much more directly. In fact, these days neutrinos, particularly muon neutrinos, can be prepared in intense beams which are scattered off hadronic, or even leptonic, targets to probe the structure of the weak interaction. A common method is to allow a high-energy monoenergetic beam of pions (or kaons) to decay (e.g., $\pi^+ \to \mu^+ \nu_\mu$) in a long decay tunnel and then to absorb the muons by passing the, approximately collinear, decay products through a thick shield which absorbs the charged particles, letting only the neutrinos through. This technological achievement opens up the possibility of exhibiting the $\gamma^\mu(1 - \gamma^5)$ structure of the weak coupling by measuring the angular distribution of $\nu_e e$ or $\bar{\nu}_e e$ scattering. This is the analogue of the confirmation of the γ^μ structure of the electromagnetic vertex by studying ee or eμ scattering, which we discussed in Chapter 6.

The relevant diagrams are shown in Fig. 12.8, where the particle four-momenta are defined. The invariant amplitude for $\nu_e e^- \to \nu_e e^-$ is computed from diagram (a):

$$\mathcal{M} = \frac{G}{\sqrt{2}} \big(\bar{u}(k')\gamma^\mu(1 - \gamma^5)u(p)\big)\big(\bar{u}(p')\gamma_\mu(1 - \gamma^5)u(k)\big). \quad (12.56)$$

The calculation now proceeds along the lines of that for $e^-\mu^-$ scattering in Section 6.3, except for the replacement of γ^μ by $\gamma^\mu(1 - \gamma^5)$. Squaring (12.56), summing over the final-state spins, and averaging over the two spin states of the

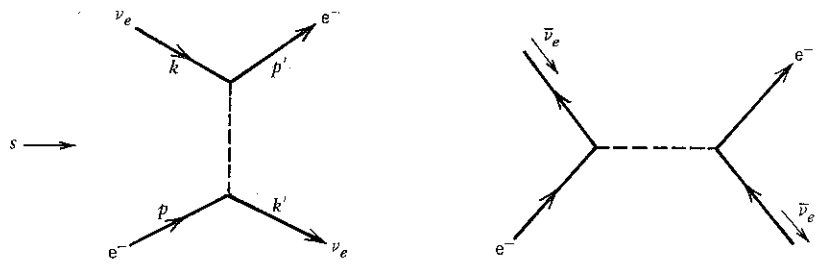

(a) Neutrino–electron scattering (b) Antineutrino–electron scattering

Fig. 12.8 Charged current contributions to elastic $\nu_e e^-$ and $\bar{\nu}_e e^-$ scattering.

initial e^- gives

$$\frac{1}{2}\sum_{\text{spins}}|\mathcal{M}|^2 = \frac{G^2}{4}\,\mathrm{Tr}\big(\gamma^\mu(1-\gamma^5)\not{p}\gamma^\nu(1-\gamma^5)\not{k}'\big)\,\mathrm{Tr}\big(\gamma_\mu(1-\gamma^5)\not{k}\gamma_\nu(1-\gamma^5)\not{p}'\big)$$

$$= 64G^2(k\cdot p)(k'\cdot p')$$

$$= 16G^2s^2 \tag{12.57}$$

where we have used (12.29). Also we are working in the relativistic limit $m_e = 0$ and have made use of

$$s = (k+p)^2 = 2k\cdot p = 2k'\cdot p'. \tag{12.58}$$

The angular distribution in the center of mass follows from (4.35) (with $p_f = p_i$ in the limit $m_e = 0$):

$$\frac{d\sigma(\nu_e e^-)}{d\Omega} = \frac{1}{64\pi^2 s}\overline{|\mathcal{M}|^2} = \frac{G^2 s}{4\pi^2}. \tag{12.59}$$

Integration over this isotropic angular distribution gives

$$\sigma(\nu_e e^-) = \frac{G^2 s}{\pi}. \tag{12.60}$$

EXERCISE 12.14 On purely dimensional grounds, show that the cross section (for a point interaction) must behave as $\sigma(\nu_e e^-) \sim G^2 s$ at high energies. Comment on the significance of this result.

EXERCISE 12.15 Show that

$$\sigma(\nu_e e^-) \approx (E_\nu \text{ in GeV}) \times 10^{-41}\ \text{cm}^2,$$

where E_ν is the laboratory energy of the neutrino.

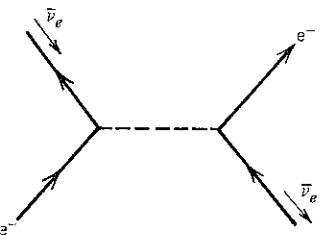

(b) Antineutrino-electron scattering

elastic $\nu_e e^-$ and $\bar{\nu}_e e^-$ scattering.

$k')\,\mathrm{Tr}\big(\gamma_\mu(1-\gamma^5)k\gamma_\nu(1-\gamma^5)p'\big)$

(12.57)

ng in the relativistic limit $m_e = 0$

$= 2k' \cdot p'.$ (12.58)

ollows from (4.35) (with $p_f = p_i$ in

$|^2 = \dfrac{G^2 s}{4\pi^2}.$ (12.59)

ion gives

. (12.60)

grounds, show that the cross ave as $\sigma(\nu_e e^-) \sim G^2 s$ at high s result.

10^{-41} cm^2,

trino.

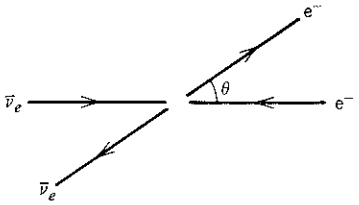

Fig. 12.9 Definition of θ for $\bar{\nu}_e e^-$ scattering.

The Feynman diagram for $\bar{\nu}_e e^- \to e^- \bar{\nu}_e$ is shown in Fig. 12.8b. We see that it can be obtained by crossing the neutrinos in $\nu_e e^- \to e^- \nu_e$ of diagram (a); see Sections 4.6 and 4.7. We therefore simply replace s by t in (12.57):

$$\frac{1}{2}\sum_{\text{spins}} |\mathcal{M}|^2 = 16G^2t^2$$

$$= 4G^2s^2(1-\cos\theta)^2, \tag{12.61}$$

where θ is the angle between the incoming $\bar{\nu}_e$ and the outgoing e^- (see Fig. 12.9), and

$$t \simeq -\frac{s}{2}(1-\cos\theta),$$

see (4.45). From (12.61), we obtain

$$\frac{d\sigma(\bar{\nu}_e e^-)}{d\Omega} = \frac{G^2 s}{16\pi^2}(1-\cos\theta)^2, \tag{12.62}$$

and integrating over angles yields

$$\sigma(\bar{\nu}_e e^-) = \frac{G^2 s}{3\pi}. \tag{12.63}$$

Comparing with (12.60) gives

$$\sigma(\bar{\nu}_e e^-) = \tfrac{1}{3}\sigma(\nu_e e^-). \tag{12.64}$$

Results (12.59), (12.62), and (12.64) expose the $\gamma^\mu(1-\gamma^5)$ structure of the weak current in a way that can be experimentally checked. We can convince ourselves of this important statement by comparing the results with those obtained for the γ^μ vertex in the electromagnetic process $e\mu \to e\mu$ or by performing the following exercise.

EXERCISE 12.16 If the weak charged current had had a structure $\gamma^\mu(a + b\gamma^5)$ show that for neutrino-electron scattering

$$\frac{d\sigma}{d\Omega} = \frac{G^2 s}{32\pi^2}\left[A^+ + A^- \cos^4\frac{\theta}{2}\right]$$

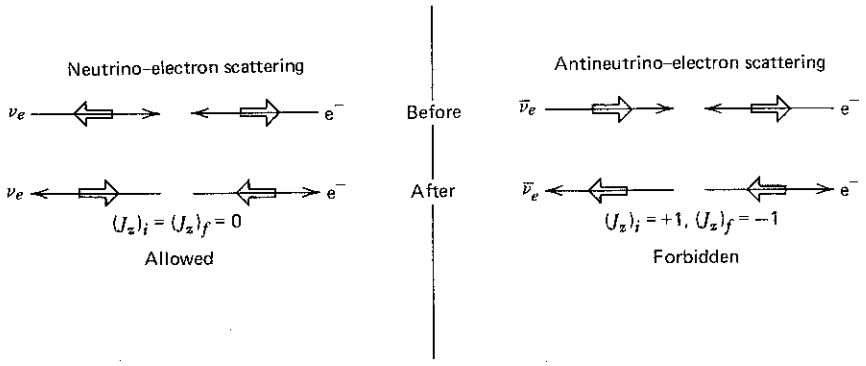

Fig. 12.10 Backward scattering in the center-of-mass frame. The long arrows represent the particle momenta and the short arrows represent their helicities in the limit in which the masses are negligible. The z axis is along the incident neutrino direction.

for both ν_ee and $\bar{\nu}_e$e elastic scattering. If this were the case, then, in contrast to (12.64), we would have

$$\sigma(\bar{\nu}_e e) = \sigma(\nu_e e).$$

The most striking difference between the two angular distributions, (12.59) and (12.62), is that $\bar{\nu}_e$e scattering vanishes for $\cos\theta = 1$, whereas ν_ee scattering does not. With our definition of θ, see Fig. 12.9, this corresponds to backward scattering of the beam particle. We could have anticipated these results from the helicity arguments we used to interpret previous calculations. The by now familiar pictures are shown in Fig. 12.10. Backward $\bar{\nu}_e$e scattering is forbidden by angular momentum conservation. In fact, the process $\bar{\nu}_e e \to \bar{\nu}_e e$ proceeds entirely in a $J = 1$ state with net helicity $+1$; that is, only one of the three helicity states is allowed. This is the origin of the factor $\frac{1}{3}$ in (12.64). With our definition of θ, the allowed amplitude is proportional to $d^1_{-11}(\theta) = \frac{1}{2}(1 - \cos\theta)$, see (6.39), in agreement with result (12.61).

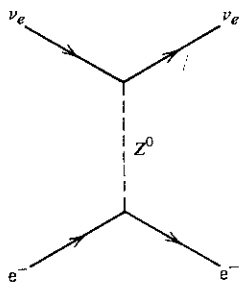

Fig. 12.11 Neutral current contributions to neutrino–electron elastic scattering.

Elastic $\nu_e e^-$ and $\bar{\nu}_e e^-$ scattering can also proceed via a weak neutral current interaction (see Fig. 12.11) which interferes with the charged current interaction (Fig. 12.8a). This is discussed in Section 13.5. However, high-energy neutrino beams are predominantly ν_μ (or $\bar{\nu}_\mu$), and so the most accessible (charged current) purely leptonic scattering process is

$$\nu_\mu + e^- \to \mu^- + \nu_e \tag{12.65}$$

(i.e., inverse muon decay). Here, there is no neutral current contribution, and so the cross section is given just by (12.59).

12.8 Neutrino–Quark Scattering

A study of the scattering of ν_μ's (or $\bar{\nu}_\mu$'s) from quarks is experimentally feasible by impinging high-energy neutrino beams on proton or nuclear targets. This is analogous to the study of the electromagnetic lepton–quark interaction by scattering high-energy electron or muon beams off hadronic targets, which we described in Chapters 8 and 9.

To predict the neutrino–quark cross sections, we clearly need to know the form of the quark weak currents. Quarks interact electromagnetically just like leptons, apart from their fractional charge. Our inclination therefore is to construct the quark weak current just as we did for leptons. For instance, we model the charge-raising quark current

$$J_q^\mu = \bar{u}_u \gamma^\mu \tfrac{1}{2}(1 - \gamma^5) u_d \quad \Longrightarrow \tag{12.66}$$

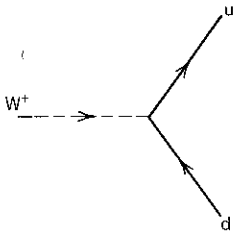

on the electron weak current (12.12)

$$J_e^\mu = \bar{u}_\nu \gamma^\mu \tfrac{1}{2}(1 - \gamma^5) u_e \quad \Longrightarrow \tag{12.67}$$

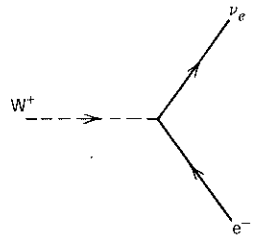

The hermitian conjugates of (12.66) and (12.67) give the charge-lowering weak currents

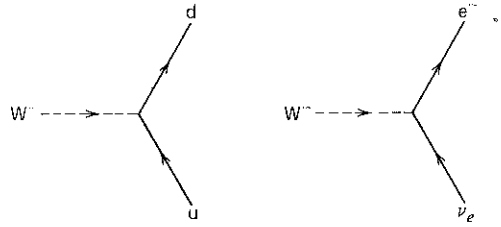

The V–A structure means that the weak current couples only left-handed u and d quarks (or right-handed $\bar{u}$ and $\bar{d}$ quarks), see Exercise 12.3. At high energies, this means only negative helicity u and d quarks are coupled, or positive helicity $\bar{u}$ and $\bar{d}$ quarks.

Using the above currents, we can evaluate diagrams such as Fig. 12.12. That is, we can calculate the amplitude for

$$d \to u e^- \bar{\nu}_e$$

which is responsible for a constituent description of neutron β-decay. The "spectator" u and d quarks, shown in Fig. 12.12, can be treated just like the spectator nucleons in the nuclear β-transitions of Section 12.3. The same $d \to u$ transition is responsible for the $\pi^- \to \pi^0 e^- \nu_e$ decay mode, the spectator quark now being a $\bar{u}$; alternatively, we may have a $\bar{u} \to \bar{d}$ transition with a spectator d quark.

EXERCISE 12.17 Using the above approach, show that

$$\Gamma(\pi^- \to \pi^0 e^- \bar{\nu}_e) = \frac{G^2}{30\pi^3}(\Delta m)^5, \tag{12.68}$$

where $\Delta m = m(\pi^-) - m(\pi^0) = 4.6$ MeV. Evaluate the decay rate and compare with $\Gamma(\pi^- \to \mu^- \bar{\nu}_\mu)$.

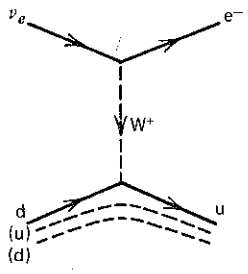

Fig. 12.12 The quark diagram responsible for neutron β-decay, $n \to p e^- \bar{\nu}_e$. The two spectator quarks which do not take part in the weak interaction are shown by dashed lines.

We are now ready to tackle neutrino–quark scattering. As the quarks and lepton weak currents have identical forms, we can carry over the results for νe scattering that we obtained in Section 12.7. From (12.59) and (12.62), we obtain in the center-of-mass frame

$$\frac{d\sigma(\nu_\mu \mathrm{d} \to \mu^- \mathrm{u})}{d\Omega} = \frac{G^2 s}{4\pi^2} \tag{12.69}$$

$$\frac{d\sigma(\bar{\nu}_\mu \mathrm{u} \to \mu^+ \mathrm{d})}{d\Omega} = \frac{G^2 s}{16\pi^2}(1 + \cos\theta)^2, \tag{12.70}$$

where θ is defined as in Fig. 12.13. From the figure, it is immediately apparent that the backward $\bar{\nu}_\mu \mathrm{u} \to \mu^+ \mathrm{d}$ scattering ($\theta = \pi$) is forbidden by helicity considerations. The cross sections for scattering from antiquarks, $\bar{\nu}_\mu \bar{\mathrm{d}} \to \mu^+ \bar{\mathrm{u}}$ and $\nu_\mu \bar{\mathrm{u}} \to \mu^- \bar{\mathrm{d}}$, are given by (12.69) and (12.70), respectively. We see that, for instance, ν_μ does not interact with either u or $\bar{\mathrm{d}}$ quarks.

To compare these results with experiment, we have to embed the constituent cross sections, (12.69) and (12.70), in the overall νN inclusive cross section. The procedure is familiar from Chapter 9. We obtain

$$\frac{d\sigma(\nu N \to \mu X)}{dx\,dy} = \sum_i$$

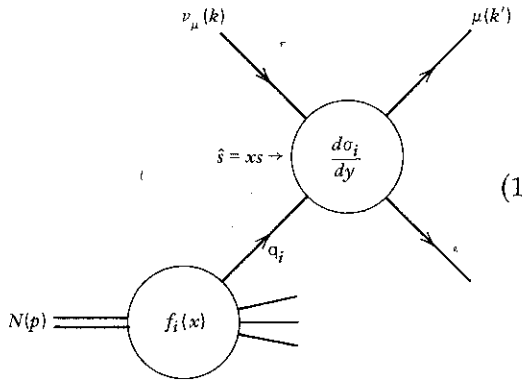

(12.71)

$$= \sum_i f_i(x)\left(\frac{d\sigma_i}{dy}\right)_{\hat{s}=xs}. \tag{12.72}$$

First, note that the angular distributions of the constituent process have been expressed in terms of the dimensionless variable y. It is related to $\cos\theta$ by

$$1 - y \equiv \frac{p \cdot k'}{p \cdot k} \simeq \tfrac{1}{2}(1 + \cos\theta),$$

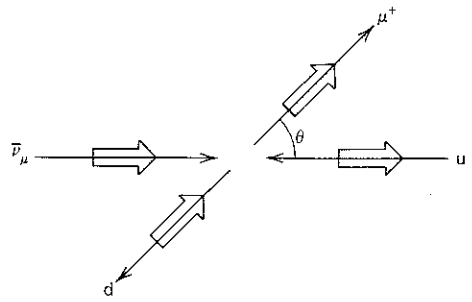

Fig. 12.13 The helicity configuration for high-energy $\bar{\nu}_\mu \mathrm{u} \to \mu^+ \mathrm{d}$ scattering.

see (9.25). The four-momenta are given in (12.71). The constituent cross sections, (12.69) and (12.70), are therefore

$$\frac{d\sigma}{dy}\left(\nu_\mu \mathrm{d} \to \mu^- \mathrm{u}\right) = \frac{G^2 xs}{\pi}, \tag{12.73}$$

$$\frac{d\sigma}{dy}\left(\bar{\nu}_\mu \mathrm{u} \to \mu^+ \mathrm{d}\right) = \frac{G^2 xs}{\pi}(1-y)^2. \tag{12.74}$$

The appropriate $\nu \mathrm{q} \to \mu \mathrm{q}'$ center-of-mass energy is xs, where now s refers to $\nu \mathrm{N} \to \mu \mathrm{X}$ (see Exercise 9.3). Using these results, together with the nucleon structure functions $f_i(x)$ introduced in Chapter 9, we can calculate the deep inelastic $\nu_\mu \mathrm{N} \to \mu \mathrm{X}$ cross section.

To confront these parton model predictions with experiment, it is simplest to take an isoscalar target, in which the nuclei contain equal numbers of protons and neutrons. The neutrinos interact only with d or $\bar{\mathrm{u}}$ quarks. They therefore measure

$$\begin{aligned} d^p(x) + d^n(x) &= d(x) + u(x) \equiv Q(x) \\ \bar{u}^p(x) + \bar{u}^n(x) &= \bar{u}(x) + \bar{d}(x) \equiv \bar{Q}(x), \end{aligned} \tag{12.75}$$

see (9.29), where we have denoted the distribution functions, $f_i(x)$, of up- and down-quarks in a proton by $u(x)$ and $d(x)$. Inserting (12.73) and the cross section for $\nu_\mu \bar{\mathrm{u}} \to \mu^- \bar{\mathrm{d}}$ into (12.72), we find the $\nu_\mu \mathrm{N} \to \mu^- \mathrm{X}$ cross section per nucleon to be

$$\frac{d\sigma}{dx\,dy}\left(\nu_\mu \mathrm{N} \to \mu^- \mathrm{X}\right) = \frac{G^2 xs}{2\pi}\left(Q(x) + (1-y)^2\,\bar{Q}(x)\right). \tag{12.76}$$

On the other hand, antineutrinos interact with $\bar{\mathrm{d}}$ and u constituents; and going through the same steps, we obtain

$$\frac{d\sigma}{dx\,dy}\left(\bar{\nu}_\mu \mathrm{N} \to \mu^+ \mathrm{X}\right) = \frac{G^2 xs}{2\pi}\left[\bar{Q}(x) + (1-y)^2\,Q(x)\right]. \tag{12.77}$$

EXERCISE 12.18 Show that deep inelastic electron electromagnetic scattering on an isoscalar target gives

$$\frac{d\sigma\,(\mathrm{eN} \to \mathrm{eX})}{dx\,dy} = \frac{2\pi\alpha^2}{Q^4} xs\left[1 + (1-y)^2\right] \frac{5}{18}\left[Q(x) + \bar{Q}(x)\right] \qquad (12.78)$$

per nucleon, see Exercise 9.5. Note that, in contrast to $\nu\mathrm{N} \to \mu\mathrm{X}$, (12.78) embodies parity conservation so Q and $\bar{Q}$ appear symmetrically.

If there were just three valence quarks in a nucleon, $\bar{Q} = 0$, the $\nu\mathrm{N} \to \mu^-\mathrm{X}$ and $\bar{\nu}\mathrm{N} \to \mu^+\mathrm{X}$ data would exhibit the dramatic V–A properties of the weak interaction exactly. That is,

$$\frac{d\sigma(\nu)}{dy} = c, \qquad \frac{d\sigma(\bar{\nu})}{dy} = c(1-y)^2, \qquad (12.79)$$

where c can be found from (12.76); and for the integrated cross sections,

$$\frac{\sigma(\bar{\nu})}{\sigma(\nu)} = \frac{1}{3}.$$

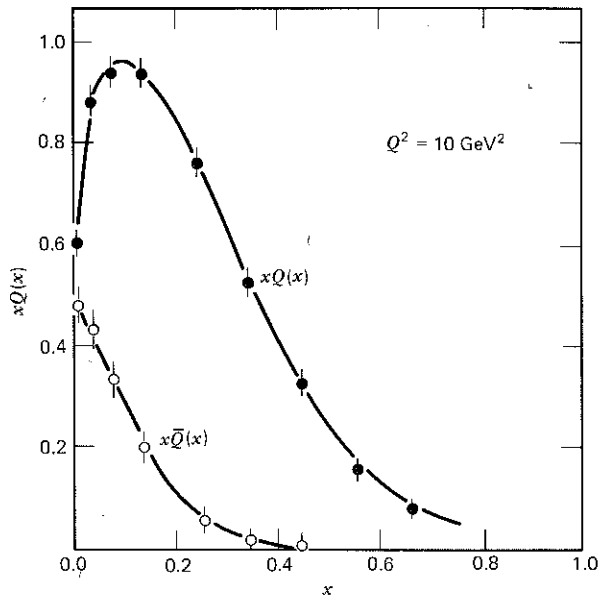

Fig. 12.14 Quark and antiquark momentum distributions in a nucleon as measured at CERN and the Fermi laboratory. The experiments reveal that only about half the proton's momentum is carried by quarks. We have associated the remainder with the gluon constituents (see Section 9.4).

The data approximately reproduce these expectations. In fact, (12.76) and (12.77) allow a determination of $Q(x)$ and $\bar{Q}(x)$. An example is shown in Fig. 12.14. There is about a 5% $\bar{Q}$ component in a proton.

EXERCISE 12.19 If $\sigma(\bar{\nu})/\sigma(\nu) = R$, show that

$$\frac{\int x\,\bar{Q}(x)\,dx}{\int x\,Q(x)\,dx} = \frac{3R-1}{3-R}.$$

Detailed analyses show that the functions $u(x)$, $d(x)$,..., are indeed the same whether one extracts them from electroproduction or neutrino experiments. This is a definitive success of the parton model: the $u(x)$, $d(x)$, describe the intrinsic structure of the hadronic target and are the same whatever experimental probe is used to determine them.

12.9 First Observation of Weak Neutral Currents

The detection in 1973 of neutrino events of the type

$$\bar{\nu}_\mu e^- \to \bar{\nu}_\mu e^-, \tag{12.80}$$

$$\left.\begin{aligned} \nu_\mu N &\to \nu_\mu X \\ \bar{\nu}_\mu N &\to \bar{\nu}_\mu X \end{aligned}\right\} \tag{12.81}$$

heralded a new chapter in particle physics. These events are evidence of a weak neutral current. Until then, no weak neutral current effects had been observed, and indeed very stringent limits had been set on the (strangeness changing) neutral current by the absence of decay modes such as

$$K^0 \to \mu^+\mu^-,$$
$$K^+ \to \pi^+ e^+ e^-,$$
$$K^+ \to \pi^+ \nu\bar{\nu}.$$

Induced weak neutral current effects are expected to occur by the combined action of the (neutral) electromagnetic and the (charged) weak current (for example, $K^+ \to \pi^+ e^+ e^-$ can proceed via a virtual photon: $K^+ \to \pi^+ \gamma$ with $\gamma \to e^+ e^-$), but these effects are very small. The rate, compared to the corresponding allowed weak decay, is of the order

$$\frac{\Gamma(K^+ \to \pi^+ e^+ e^-)}{\Gamma(K^+ \to \pi^0 e^+ \nu_e)} \sim \left(\frac{\alpha G}{G}\right)^2 \sim 10^{-5}, \tag{12.82}$$

in agreement with the data. (Here, the $1/q^2$ behavior of the propagator of the virtual photon is canceled by the helicity suppression of the $0^- \to 0^-\gamma$ coupling.)

However, reactions (12.80) and (12.81) were found to occur at rates very similar to those of other weak scattering processes.

12.10 Neutral Current Neutrino–Quark Scattering

A quantitative comparison of the strength of neutral current (NC) to charged current (CC) weak processes has been obtained, for example, by scattering neutrinos off an iron target. The present experimental values are

$$R_\nu \equiv \frac{\sigma^{NC}(\nu)}{\sigma^{CC}(\nu)} \equiv \frac{\sigma(\nu_\mu \mathrm{N} \to \nu_\mu \mathrm{X})}{\sigma(\nu_\mu \mathrm{N} \to \mu^- \mathrm{X})} = 0.31 \pm 0.01,$$
$$R_{\bar\nu} \equiv \frac{\sigma^{NC}(\bar\nu)}{\sigma^{CC}(\bar\nu)} \equiv \frac{\sigma(\bar\nu_\mu \mathrm{N} \to \bar\nu_\mu \mathrm{X})}{\sigma(\bar\nu_\mu \mathrm{N} \to \mu^+ \mathrm{X})} = 0.38 \pm 0.02. \tag{12.83}$$

The $\nu\mathrm{N} \to \nu\mathrm{X}$ data can be explained in terms of neutral current–current $\nu\mathrm{q} \to \nu\mathrm{q}$ interactions, see Fig. 12.15, with amplitudes

$$\mathfrak{M} = \frac{G_N}{\sqrt{2}}\left[\bar u_\nu \gamma^\mu (1-\gamma^5) u_\nu\right]\left[\bar u_q \gamma_\mu \left(c_V^q - c_A^q \gamma^5\right) u_q\right] \tag{12.84}$$

where $q = \mathrm{u}, \mathrm{d}, \ldots$ are the quarks in the target. *A priori*, there is no reason why the neutral weak interaction should have the four-vector current–current form of (12.84). It is decided by experiment, for instance, by the observed y distribution (see Exercise 12.20).

It is appropriate at this stage to introduce the conventional normalization of the weak neutral currents, J_μ^{NC}. The invariant amplitude for an arbitrary neutral current process is written

$$\boxed{\mathfrak{M} = \frac{4G}{\sqrt{2}} 2\rho J_\mu^{NC} J^{NC\mu},} \tag{12.85}$$

compare (12.13) for a charged current process. The $\nu\mathrm{q} \to \nu\mathrm{q}$ amplitude of (12.84)

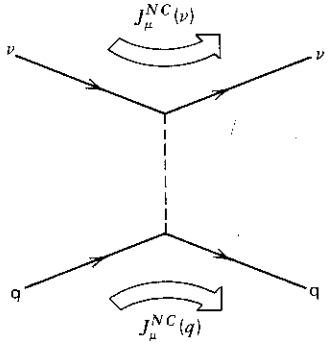

Fig. 12.15 Neutral current $\nu\mathrm{q} \to \nu\mathrm{q}$ scattering.

is of this form; the customary definition of the neutral currents is

$$J_\mu^{NC}(\nu) = \tfrac{1}{2}\left(\bar{u}_\nu \gamma_\mu \tfrac{1}{2}(1-\gamma^5)u_\nu\right), \tag{12.86}$$

$$J_\mu^{NC}(q) = \left(\bar{u}_q \gamma_\mu \tfrac{1}{2}\left(c_V^q - c_A^q \gamma^5\right)u_q\right). \tag{12.87}$$

In general, the J_μ^{NC}, unlike the charged current J_μ, are not pure V–A currents ($c_V \neq c_A$); they have right-handed components. However, the neutrino is left-handed; and so, $c_V^\nu = c_A^\nu \equiv \frac{1}{2}$ in (12.86). The parameter ρ in (12.85) determines the relative strength of the neutral and charged current processes. In the standard theoretical model all the c_V^i, c_A^i (with $i = \nu, \mathrm{e}, \mathrm{u}\ldots$) are given in terms of one parameter, and $\rho = 1$ (see Chapters 13 and 15). In other words, if the model is successful, all neutral current phenomena will be described by a common parameter. In fact, the present experiments give $\rho = 1$ to within small errors. However, for the moment let us leave c_V^i, c_A^i and ρ as free parameters to be determined by experiment. Upon inserting the currents (12.86) and (12.87) into (12.85), we obtain the $\nu\mathrm{q} \to \nu\mathrm{q}$ amplitude of (12.84) with

$$G_N = \rho G (\simeq G). \tag{12.88}$$

We now return to our interpretation of the $\nu\mathrm{N} \to \nu\mathrm{X}$ data. The calculation of the $\nu\mathrm{q} \to \nu\mathrm{q}$ cross sections proceeds exactly as that for the charged current processes $\nu\mathrm{q} \to \mu\mathrm{q}'$. For example, using the results (12.73) and (12.74),

$$\frac{d\sigma(\nu_L \mathrm{d}_L \to \mu\mathrm{u})}{dy} = \frac{G^2 x s}{\pi},$$

$$\frac{d\sigma(\nu_L \bar{\mathrm{u}}_R \to \mu\bar{\mathrm{d}})}{dy} = \frac{G^2 x s}{\pi}(1-y)^2, \tag{12.89}$$

we obtain directly

$$\frac{d\sigma(\nu\mathrm{q} \to \nu\mathrm{q})}{dy} = \frac{G_N^2 x s}{\pi}\left(\left(g_L^q\right)^2 + \left(g_R^q\right)^2 (1-y)^2\right), \tag{12.90}$$

where we have introduced

$$g_L^q \equiv \tfrac{1}{2}\left(c_V^q + c_A^q\right), \qquad g_R^q \equiv \tfrac{1}{2}\left(c_V^q - c_A^q\right). \tag{12.91}$$

As compared to (12.89), the new feature of (12.90) is the possibility of a right-handed component g_R^q of $J_\mu^{NC}(q)$.

EXERCISE 12.20 Show that $|\mathcal{M}(\nu\mathrm{q} \to \nu\mathrm{q})|^2$ behaves like s^2, $s^2(1-y)^2$, $s^2 y^2$ for pure $V-A$, pure $V+A$, and S, P neutral couplings of the quark, respectively. Pure $V \pm A$ denote $\gamma^\mu(1 \pm \gamma^5)$ couplings, and S, P stands for the scalar, pseudoscalar interaction amplitude

$$\mathcal{M} = \frac{G_N}{\sqrt{2}}\left(\bar{u}_\nu(1-\gamma^5)u_\nu\right)\left(\bar{u}_q\left(g_S - g_P\gamma^5\right)u_q\right).$$

The parton model predictions for the neutral current (NC) processes $\nu N \to \nu X$ and $\bar{\nu} N \to \bar{\nu} X$ are obtained by following the calculation of the CC processes $\nu N \to \mu^- X$ and $\bar{\nu} N \to \mu^+ X$ of Section 12.8. For an isoscalar target, we find that the cross section per nucleon is

$$\frac{d\sigma(\nu N \to \nu X)}{dx\,dy} = \frac{G_N^2 xs}{2\pi}\Big[g_L^2\big(Q(x) + (1-y)^2 \bar{Q}(x)\big) + g_R^2\big(\bar{Q}(x) + (1-y)^2 Q(x)\big)\Big], \tag{12.92}$$

where, if we assume only u, d, $\bar{\text{u}}$, $\bar{\text{d}}$ quarks within the nucleon,

$$g_L^2 \equiv \big(g_L^u\big)^2 + \big(g_L^d\big)^2, \tag{12.93}$$

and similarly for g_R^2. We may integrate over x and define

$$Q \equiv \int x\,Q(x)\,dx \doteq \int x\big[u(x) + d(x)\big]\,dx, \tag{12.94}$$

see (12.75). Cross section (12.92) and that for $\bar{\nu} N \to \bar{\nu} X$ become

$$\begin{aligned} \frac{d\sigma^{NC}(\nu)}{dy} &= \frac{G_N^2 s}{2\pi}\Big\{ g_L^2\big(Q + (1-y)^2 \bar{Q}\big) + g_R^2\big(\bar{Q} + (1-y^2) Q\big)\Big\}, \\ \frac{d\sigma^{NC}(\bar{\nu})}{dy} &= \frac{G_N^2 s}{2\pi}\Big\{ g_L^2\big(\bar{Q} + (1-y)^2 Q\big) + g_R^2\big(Q + (1-y^2) \bar{Q}\big)\Big\}, \end{aligned} \tag{12.95}$$

which are to be contrasted with the charged current expressions (12.76) and (12.77)

$$\begin{aligned} \frac{d\sigma^{CC}(\nu)}{dy} &= \frac{G^2 s}{2\pi}\big(Q + (1-y)^2 \bar{Q}\big), \\ \frac{d\sigma^{CC}(\bar{\nu})}{dy} &= \frac{G^2 s}{2\pi}\big(\bar{Q} + (1-y)^2 Q\big). \end{aligned} \tag{12.96}$$

Correcting (12.95) and (12.96) for the neutron excess in an iron target and for an s quark contribution, the present data give

$$g_L^2 = 0.300 \pm 0.015, \qquad g_R^2 = 0.024 \pm 0.008. \tag{12.97}$$

The experimental verdict is that the weak neutral current is predominantly V–A (i.e., left-handed) but, since $g_R \neq 0$, not pure V–A. The NC and the CC have a tantalizingly similar structure, but the CC is believed to have a pure V–A form. Chapter 13 takes up this point, but first we must look more carefully at the quark sector.

12.11 The Cabibbo Angle

So far, we have seen that leptons and quarks participate in weak interactions through charged V–A currents constructed from the following pairs of (left-

handed) fermion states:

$$\begin{pmatrix} \nu_e \\ e^- \end{pmatrix}, \qquad \begin{pmatrix} \nu_\mu \\ \mu^- \end{pmatrix}, \qquad \text{and} \qquad \begin{pmatrix} u \\ d \end{pmatrix}. \tag{12.98}$$

All these charged currents couple with a universal coupling constant G. It is natural to attempt to extend this universality to embrace the doublet

$$\begin{pmatrix} c \\ s \end{pmatrix} \tag{12.99}$$

formed from the heavier quark states. However, we already know that this cannot be quite correct. For instance, the decay $K^+ \to \mu^+ \nu_\mu$ occurs. The K^+ is made of u and $\bar{s}$ quarks. There must thus be a weak current which couples a u to an $\bar{s}$ quark (see Fig. 12.16). This contradicts the above scheme, which only allows weak transitions between u $\leftrightarrow$ d and c $\leftrightarrow$ s.

Instead of introducing new couplings to accommodate observations like $K^+ \to \mu^+ \nu_\mu$, let us try to keep universality but modify the quark doublets. We assume that the charged current couples "rotated" quark states

$$\begin{pmatrix} u \\ d' \end{pmatrix}, \qquad \begin{pmatrix} c \\ s' \end{pmatrix}, \ldots, \tag{12.100}$$

where

$$\begin{aligned} d' &= d \cos\theta_c + s \sin\theta_c \\ s' &= -d \sin\theta_c + s \cos\theta_c. \end{aligned} \tag{12.101}$$

This introduces an arbitrary parameter θ_c, the quark mixing angle, known as the Cabibbo angle. In 1963, Cabibbo first introduced the doublet u, d′ to account for the weak decays of strange particles. Indeed, the mixing of the d and s quark can be determined by comparing $\Delta S = 1$ and $\Delta S = 0$ decays. For example,

$$\frac{\Gamma(K^+ \to \mu^+ \nu_\mu)}{\Gamma(\pi^+ \to \mu^+ \nu_\mu)} \sim \sin^2\theta_c,$$

$$\frac{\Gamma(K^+ \to \pi^0 e^+ \nu_e)}{\Gamma(\pi^+ \to \pi^0 e^+ \nu_e)} \sim \sin^2\theta_c.$$

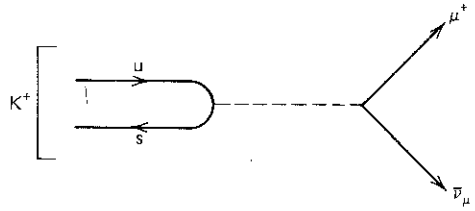

Fig. 12.16 The decay $K^+ \to \mu^+ \bar{\nu}_\mu$.

After allowing for the kinematic factors arising from the different particle masses, the data show that the $\Delta S = 1$ transitions are suppressed by a factor of about 20 as compared to the $\Delta S = 0$ transitions. This corresponds to a Cabibbo angle $\theta_c \approx 13°$.

What we have done is to change our mind about the charged current (12.66). We now have "Cabibbo favored" transitions (proportional to $\cos\theta_c$)

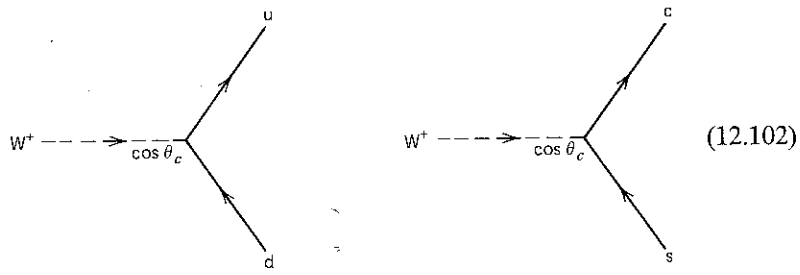

(12.102)

and "Cabibbo suppressed" transitions

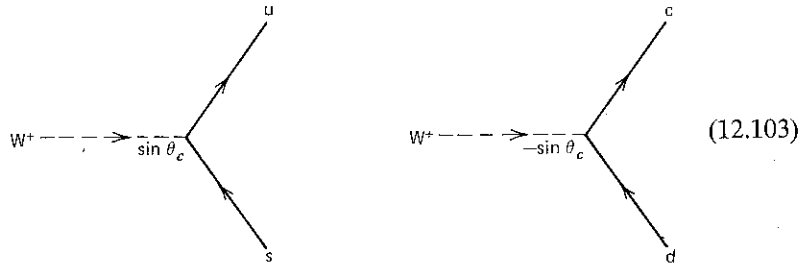

(12.103)

[see (12.101)], and similar diagrams for the charge-lowering transitions. We can summarize this by writing down the explicit form of the matrix element describing the charged current weak interactions of the quarks. From (12.13),

$$\mathcal{M} = \frac{4G}{\sqrt{2}} J^\mu J_\mu^\dagger \tag{12.104}$$

with

$$J^\mu = (\bar{u} \quad \bar{c}) \frac{\gamma^\mu(1-\gamma^5)}{2} U \begin{pmatrix} d \\ s \end{pmatrix}. \tag{12.105}$$

The unitary matrix U performs the rotation (12.101) of the d and s quark states:

$$U = \begin{pmatrix} \cos\theta_c & \sin\theta_c \\ -\sin\theta_c & \cos\theta_c \end{pmatrix}. \tag{12.106}$$

Of course, there will also be amplitudes describing semileptonic decays constructed from the product of a quark with a lepton current, $J^\mu(\text{quark})\, J_\mu^\dagger(\text{lepton})$.

All this has implications for our previous calculations. For instance, we must replace G in the formula for the nuclear β-decay rate by

$$G_\beta = G\cos\theta_c, \tag{12.107}$$

whereas the purely leptonic μ-decay rate, which involves no mixing, is unchanged: $G_\mu = G$. The detailed comparison of these rates, (12.44), supports Cabibbo's hypothesis.

The weak interactions discussed so far involve only the u and d′ quark states. However, in (12.100), we have coupled s′ to the charmed quark c, so that we have weak transitions c ↔ s′ as well as d′ ↔ u. In fact, following this line of argument, Glashow, Iliopoulos, and Maiani (GIM) proposed the existence of the c quark some years before its discovery. A reason for doing this can be seen by studying the decay $K^0 \to \mu^+\mu^-$. With only u ↔ d′ transitions, the diagram of Fig. 12.17a predicts that the $K_L^0 \to \mu^+\mu^-$ decay would occur at a rate far in excess of what is observed:

$$\frac{\Gamma(K_L^0 \to \mu^+\mu^-)}{\Gamma(K_L^0 \to \text{all modes})} = (9.1 \pm 1.9) \times 10^{-9}.$$

However, with the introduction of the c quark, a second diagram, Fig. 12.17b, occurs which would exactly cancel with diagram 12.17a if it were not for the mass difference of the u and c quarks. We take up this discussion in the next section.

The c, s′ weak current is responsible for the weak decays of charmed particles. A delightful example is the decay of a D^+ meson. The D^+ meson consists of a c and $\bar{d}$ quark. Since $\cos^2\theta_c \gg \sin^2\theta_c$, it follows from (12.100) and (12.101) that the favored quark decay pattern is that shown in Fig. 12.18, with amplitude

$$\mathcal{M}(c \to s\bar{u}d) \sim \cos^2\theta_c. \tag{12.108}$$

That is, a $\bar{K}$ meson should preferentially feature among the decay products of a D^+. On the other hand, the decay $D^+ \to K \ldots$ is highly (Cabibbo) suppressed since

$$\mathcal{M}(c \to \bar{s}ud) \sim \sin^2\theta_c. \tag{12.109}$$

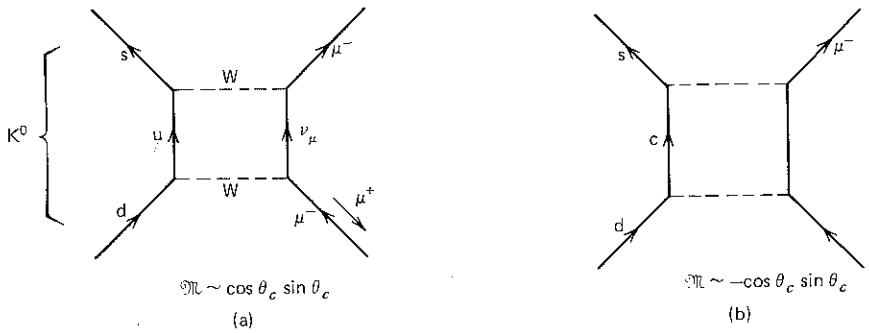

Fig. 12.17 Two contributions to $K^0 \to \mu^+\mu^-$. Diagram (b) is simply (a) with u → c.

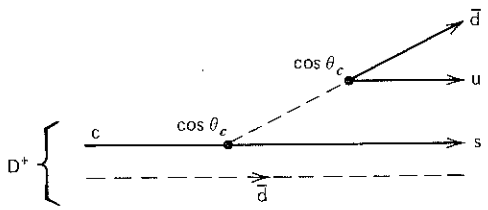

Fig. 12.18 A quark description of D^+ decay: the Cabibbo-favored process is $c \to s u \bar{d}$ with a spectator $\bar{d}$ quark.

We thus have a very characteristic signature for D^+ decay, that for instance the decay mode $K^-\pi^+\pi^+$ is highly favored as compared to the $K^+\pi^+\pi^-$ mode.

EXERCISE 12.21 Estimate the relative rates for the following three decay modes of the $D^0(c\bar{u})$ meson: $D^0 \to K^-\pi^+$, $\pi^-\pi^+$, $K^+\pi^-$.

EXERCISE 12.22 Given that the partial rate

$$\Gamma(K^+ \to \pi^0 e^+ \nu) = 4 \times 10^6 \text{ sec}^{-1},$$

calculate the rate for $D^0 \to K^- e^+ \nu$. Hence, estimate the lifetime of the D^0 meson.

EXERCISE 12.23 Show, in the "spectator" quark model approach, that the charmed meson lifetimes satisfy

$$\tau(D^0) = \tau(D^+) = \tau(F^+),$$

where F^+ is made of c and $\bar{s}$ quarks, see Chapter 2.

12.12 Weak Mixing Angles

We can summarize the above Cabibbo-GIM scheme as follows. The charged (or flavor-changing) current couples $u \leftrightarrow d'$ or $c \leftrightarrow s'$ (left-handed) quark states, where d' and s' are orthogonal combinations of the physical (i.e., mass) eigenstates of quarks of definite flavor d, s:

$$\begin{pmatrix} d' \\ s' \end{pmatrix} = \begin{pmatrix} \cos\theta_c & \sin\theta_c \\ -\sin\theta_c & \cos\theta_c \end{pmatrix} \begin{pmatrix} d \\ s \end{pmatrix}. \tag{12.110}$$

The quark mixing is described by a single parameter, the Cabibbo angle θ_c.

The original motivation for the GIM proposal was to ensure that there are no $s \leftrightarrow d$ transitions, which change flavor but not charge. The experimental evidence for the absence of strangeness-changing neutral currents is compelling. For

instance, decays such as $K^0 \to \mu^+\mu^-$, $K^+ \to \pi^+ e^+ e^-$, $K^+ \to \pi^+ \nu\bar{\nu}$, which would be otherwise allowed, are either absent or highly suppressed.

How does the GIM mechanism work? To see this, it is convenient to rewrite (12.110) in the form

$$d_i' = \sum_j U_{ij} d_j, \tag{12.111}$$

with $d_1 \equiv d_L$ and $d_2 \equiv s_L$ where L denotes a left-handed quark state. Now the matrix U, introduced in (12.105), is unitary (provided we adopt the universal weak coupling hypothesis), and therefore we have

$$\begin{aligned} \sum_i \bar{d}_i' d_i' &= \sum_{i,j,k} \bar{d}_j U_{ji}^\dagger U_{ik} d_k \\ &= \sum_j \bar{d}_j d_j. \end{aligned} \tag{12.112}$$

That is, only transitions $d \to d$ and $s \to s$ are allowed; flavor-changing transitions, $s \leftrightarrow d$, are forbidden.

Before we extend the GIM mechanism to incorporate additional quark flavors, we must answer two questions that may have come to mind. First, why is the mixing taken in the d, s sector? In fact, the mixing could equally well have been formulated in the u, c sector; no observable difference would result since the absolute phases of the quark wavefunctions are not observable. Indeed, a more involved mixing in both the u, c and d, s sectors can be used, but it can always be simplified (by appropriately choosing the phases of the quark states) to the one-parameter form given in (12.110). This will become clearer in a moment.

A second question is, "Why is there no Cabibbo-like angle in the leptonic sector?"

$$\begin{pmatrix} \nu_e \\ e^- \end{pmatrix}, \quad \begin{pmatrix} \nu_\mu \\ \mu^- \end{pmatrix}. \tag{12.113}$$

The reason is that if ν_e and ν_μ are massless, then lepton mixing is unobservable. Any Cabibbo-like rotation still leaves us with neutrino mass eigenstates. By definition, we take ν_e to be the partner of the electron. This guarantees conserved lepton numbers L_e and L_μ. By contrast, the weak interaction eigenstates d', s' are not the same as the mass eigenstates but are related by (12.110).

Now consider the generalization of the Cabibbo-GIM ideas to more than four quark flavors. Imagine for a moment that weak interactions operate on N doublets of left-handed quarks,

$$\begin{pmatrix} u_i \\ d_i' \end{pmatrix} \qquad \text{with } i = 1, 2, \ldots, N \tag{12.114}$$

where d_i' are mixtures of the mass eigenstates d_i:

$$d_i' = \sum_{j=1}^{N} U_{ij} d_j. \tag{12.115}$$

U is a unitary $N \times N$ matrix to be determined by the flavor-changing weak processes. How many observable parameters does U contain? We can change the phase of each of the $2N$ quark states independently without altering the physics. Therefore, U contains

$$N^2 - (2N - 1)$$

real parameters. One phase is omitted as an overall phase change still leaves U invariant. On the other hand, an orthogonal $N \times N$ matrix has only $\frac{1}{2}N(N-1)$ real parameters [e.g., (12.110)]. Therefore, by redefining the quark phases, it is not possible, in general, to make U real. U must contain

$$N^2 - (2N - 1) - \tfrac{1}{2}N(N-1) = \tfrac{1}{2}(N-1)(N-2) \qquad (12.116)$$

residual phase factors. Thus, for two doublets ($N = 2$), there is one real parameter (θ_c), whereas for three doublets, there are three real parameters and one phase factor, $e^{i\delta}$.

We have in fact conclusive evidence for a fifth flavor of quark, the bottom quark b with charge $Q = -\frac{1}{3}$ (see Chapter 2), and it is widely believed that its partner, the top quark t with $Q = +\frac{2}{3}$, exists. Weak interactions would then operate on three doublets of left-handed quarks,

$$\begin{pmatrix} u \\ d' \end{pmatrix}, \quad \begin{pmatrix} c \\ s' \end{pmatrix}, \quad \begin{pmatrix} t \\ b' \end{pmatrix}. \qquad (12.117)$$

Why should we expect quarks to come in pairs? There are two reasons for this. First, it provides a natural way to suppress the flavor-changing neutral current; the argument leading to (12.112) applies just as well for three as for two doublets. The second reason is concerned with the desire to obtain a renormalizable gauge theory of weak interactions (see Chapters 14 and 15). This requires a delicate cancellation between different diagrams, relations which can easily be upset by "anomalies" due to fermion loops such as Fig. 12.19. These anomalies must be canceled for a renormalizable theory. Each triangle is proportional to $c_A^f Q_f^2$, where Q_f is the charge and c_A^f is the axial coupling of the weak neutral current. Thus, for an equal number N of lepton and quark doublets, the total anomaly is proportional to

$$\sum_{i=1}^{N} \left(\tfrac{1}{2}(0)^2 - \tfrac{1}{2}(-1)^2 + \tfrac{1}{2}N_c\left(+\tfrac{2}{3}\right)^2 - \tfrac{1}{2}N_c\left(-\tfrac{1}{3}\right)^2 \right) = 0. \qquad (12.118)$$

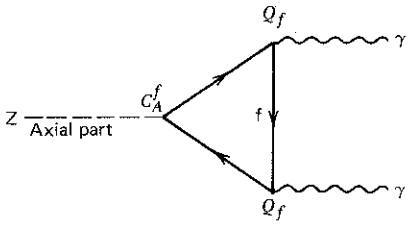

Fig. 12.19 A fermion (quark or lepton) triangle diagram which potentially could cause an anomaly.

The values used for c_A^f are determined in the next chapter (see Table 13.2). Thus, taking account of the three colors of each quark ($N_c = 3$), the anomalies are canceled. Since we have three lepton doublets (electron, muon, and tau), it is therefore natural to anticipate the three quark doublets of (12.117).

It is straightforward to extend the weak current, (12.105), to embrace the new doublet of quarks:

$$J^\mu = (\bar{u}\,\bar{c}\,\bar{t})\frac{\gamma_\mu(1-\gamma^5)}{2}U\begin{pmatrix} d \\ s \\ b \end{pmatrix}. \tag{12.119}$$

The 3×3 mixing matrix U contains three real parameters (Cabibbo-like mixing angles) and a phase factor $e^{i\delta}$ [see (12.116)]. The original parametrization was due to Kobayashi and Maskawa. Due to the phase δ, the matrix U is complex, unlike the 2×2 matrix of (12.110). That is, with the discovery of the b quark, complex elements U_{ij} enter the weak current. This has fundamental implications concerning CP invariance, which we discuss in the next section.

We illustrated how each element of the 2×2 Cabibbo matrix can be determined from experimental information on the corresponding quark flavor transition. The elements of the 3×3 matrix can also be studied in the same way. The present status of the experimental situation may be summarized as follows:

$$U = \begin{bmatrix} |U_{ud}| = 0.973 & |U_{us}| = 0.23 & |U_{ub}| \simeq 0 \\ |U_{cd}| \simeq 0.24 & |U_{cs}| \simeq 0.97 & |U_{cb}| \simeq 0.06 \\ |U_{td}| \simeq 0 & |U_{ts}| \simeq 0 & |U_{tb}| \simeq 1 \end{bmatrix}. \tag{12.120}$$

where $|U| \simeq 0$ means that the element is very small, but not yet determined. It is not surprising that some elements are not known, since there is no experimental information on the t quark. An incomplete sketch of how the results of (12.120) are obtained is shown in Table 12.1. The most striking feature of (12.120) is that the diagonal elements U_{ud}, U_{cs}, U_{tb} are clearly dominant. The large value of $|U_{cs}|$ simply reflects the experimental fact that charm particles preferentially decay into strange particles. The experimental observation that B mesons prefer to decay into charm particles implies $|U_{cb}| > |U_{ub}|$. Moreover (12.120) indicates that T mesons (when found) should preferentially decay into B mesons. All this has interesting consequences for the study of heavy quark states or for their detection in the case of T mesons. Spectacular experimental signatures result from the favored "cascade" decays, which may be characterized by the presence of multiple leptons (or strange particles) in the final state, for example:

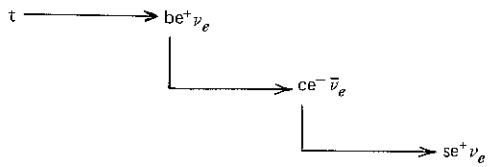

TABLE 12.1
A Summary of the Determination of the Elements $U_{qq'}$ of the Kobayashi–Maskawa Matrix

Element	Experimental Information
U_{ud}	β-Decay, generalize (12.107)
U_{us}	$K \to \pi e \nu$ and semileptonic hyperon decays, generalize discussion following (12.101)
U_{ub}	$b \to u e^- \bar{\nu}_e$, look for B meson decays with no K's in final state: gives $\lvert U_{ub}\rvert^2 < 0.02 \lvert U_{cb}\rvert^2$.
U_{cd}	$\nu_\mu d \to \mu^- c$, charmed particle production by neutrinos
U_{cs}	$\nu_\mu s \to \mu^- c$ and $D^+ \to \bar{K}^0 e^+ \nu_e$, see (12.108); also constrained by the unitarity of U, which implies $\lvert U_{cd}\rvert^2 + \lvert U_{cs}\rvert^2 + \lvert U_{cb}\rvert^2 = 1$, together with the information on $\lvert U_{cd}\rvert$ and $\lvert U_{cb}\rvert$.
U_{cb}	The (long) lifetime of the B meson, $\tau_B \sim 10^{-12}$ secs, and $\lvert U_{ub}\rvert$.
U_{tq}	From unitarity bounds

12.13 *CP* Invariance?

To investigate *CP* invariance, we first compare the amplitude for a weak process, say, the quark scattering process $ab \to cd$, with that for the antiparticle reaction $\bar{a}\bar{b} \to \bar{c}\bar{d}$. We take $ab \to cd$ to be the charged current interaction of Fig. 12.20a. The amplitude

$$\begin{aligned}\mathcal{M} &\sim J^{\mu}_{ca} J^{\dagger}_{\mu bd} \\ &\sim \left(\bar{u}_c \gamma^{\mu}(1-\gamma^5) U_{ca} u_a\right)\left(\bar{u}_b \gamma_{\mu}(1-\gamma^5) U_{bd} u_d\right)^{\dagger} \\ &\sim U_{ca} U^*_{db}\left(\bar{u}_c \gamma^{\mu}(1-\gamma^5) u_a\right)\left(\bar{u}_d \gamma_{\mu}(1-\gamma^5) u_b\right), \end{aligned} \tag{12.121}$$

since $U^{\dagger}_{bd} = U^*_{db}$. $\mathcal{M}$ describes either $ab \to cd$ or $\bar{c}\bar{d} \to \bar{a}\bar{b}$ (remembering the antiparticle description of Chapter 3).

On the other hand, the amplitude $\mathcal{M}'$ for the antiparticle process $\bar{a}\bar{b} \to \bar{c}\bar{d}$ (or $cd \to ab$) is

$$\begin{aligned}\mathcal{M}' &\sim \left(J^{\mu}_{ca}\right)^{\dagger} J_{\mu bd} \\ &\sim U^*_{ca} U_{db}\left(\bar{u}_a \gamma^{\mu}(1-\gamma^5) u_c\right)\left(\bar{u}_b \gamma_{\mu}(1-\gamma^5) u_d\right); \end{aligned} \tag{12.122}$$

that is,

$$\mathcal{M}' = \mathcal{M}^{\dagger}.$$

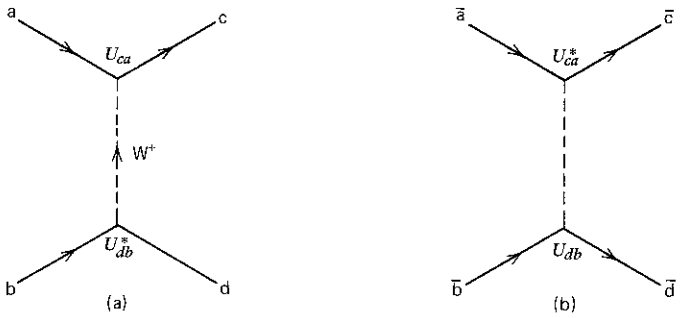

Fig. 12.20 The processes described by (a) the weak amplitude $\mathfrak{M}(ab \to cd)$ and (b) its hermitian conjugate.

This should not be surprising. It is demanded by the hermicity of the Hamiltonian. By glancing back at (4.6) and (4.17), we see that $\mathfrak{M}$ is essentially the interaction Hamiltonian V for the process. The total interaction Hamiltonian must contain $\mathfrak{M} + \mathfrak{M}^\dagger$, where $\mathfrak{M}$ describes the $i \to f$ transition and $\mathfrak{M}^\dagger$ describes the $f \to i$ transition in the notation of Chapter 4.

In Section 12.1, we have seen that weak interactions violate both P invariance and C invariance, but have indicated that invariance under the combined CP operation may hold. How do we verify that the theory is CP invariant? We calculate from $\mathfrak{M}(ab \to cd)$ of (12.121) the amplitude $\mathfrak{M}_{CP}$, describing the CP-transformed process, and see whether or not the Hamiltonian remains hermitian. If it does, that is, if

$$\mathfrak{M}_{CP} = \mathfrak{M}^\dagger,$$

then the theory is CP invariant. If it does not, then CP is violated.

$\mathfrak{M}_{CP}$ is obtained by substituting the CP-transformed Dirac spinors in (12.121):

$$u_i \to P(u_i)_C, \qquad i = a, \ldots, d \tag{12.123}$$

where u_C are the charge-conjugate spinors of Section 5.4,

$$u_C = C\bar{u}^T. \tag{12.124}$$

Clearly, to form $\mathfrak{M}_{CP}$, we need $\bar{u}_C$ and, also, to know how $\gamma^\mu(1 - \gamma^5)$ transforms under C. In the standard representation of the γ-matrices, we have [see (5.39)]

$$\begin{aligned} \bar{u}_C &= -u^T C^{-1}, \\ C^{-1}\gamma^\mu C &= -(\gamma^\mu)^T, \\ C^{-1}\gamma^\mu\gamma^5 C &= +(\gamma^\mu\gamma^5)^T. \end{aligned} \tag{12.125}$$

EXERCISE 12.24 Verify (12.125) using (5.39).

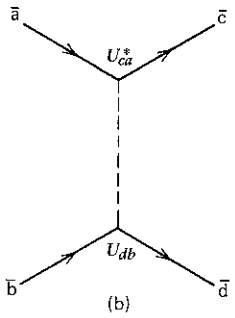

(b)

) the weak amplitude
e.

the hermicity of the Hamilto-
see that $\mathfrak{M}$ is essentially the
total interaction Hamiltonian
$\to f$ transition and $\mathfrak{M}^\dagger$ describes

ctions violate both P invariance
iance under the combined CP
e theory is CP invariant? We
nplitude $\mathfrak{M}_{CP}$, describing the
he Hamiltonian remains hermi-

en CP is violated.
rmed Dirac spinors in (12.121):

$\ldots, d$ (12.123)

ion 5.4,

(12.124)

ow how $\gamma^\mu(1-\gamma^5)$ transforms
natrices, we have [see (5.39)]

,

,

$)^T$. (12.125)

).

With the replacements (12.123), the first charged current of (12.121) becomes

$$\begin{aligned}(J^\mu_{ca})_C &= U_{ca}(\bar{u}_c)_C\,\gamma^\mu(1-\gamma^5)(u_a)_C \\ &= -U_{ca}u_c^T C^{-1}\gamma^\mu(1-\gamma^5)C\bar{u}_a^T \\ &= U_{ca}u_c^T\left[\gamma^\mu(1+\gamma^5)\right]^T\bar{u}_a^T \\ &= (-)U_{ca}\bar{u}_a\,\gamma^\mu(1+\gamma^5)u_c. \end{aligned} \tag{12.126}$$

The above procedure is exactly analogous to that used to obtain the charge-conjugate electromagnetic current, (5.40).

The parity operation $P = \gamma^0$, see (5.62), and so

$$P^{-1}\gamma^\mu(1+\gamma^5)P = \gamma^{\mu\dagger}(1-\gamma^5),$$

see (5.9)–(5.11). Thus,

$$(J^\mu_{ca})_{CP} = (-)U_{ca}\bar{u}_a\,\gamma^{\mu\dagger}(1-\gamma^5)u_c,$$

and hence

$$\mathfrak{M}_{CP} \sim U_{ca}U^*_{db}\left[\bar{u}_a\,\gamma^\mu(1-\gamma^5)u_c\right]\left[\bar{u}_b\gamma_\mu(1-\gamma^5)u_d\right]. \tag{12.127}$$

We can now compare $\mathfrak{M}_{CP}$ with $\mathfrak{M}^\dagger$ of (12.122). Provided the elements of the matrix U are real, we find

$$\mathfrak{M}_{CP} = \mathfrak{M}^\dagger,$$

and the theory is CP invariant. At the four-quark (u, d, c, s) level, this is the case, as the 2×2 matrix U, (12.106), is indeed real. However, with the advent of the b (and t) quarks, the matrix U becomes the 3×3 Kobayashi–Maskawa (KM) matrix. It now contains a complex phase factor $e^{i\delta}$. Then, in general, we have

$$\mathfrak{M}_{CP} \neq \mathfrak{M}^\dagger,$$

and the theory necessarily violates CP invariance.

In fact, a tiny CP violation had been established many years before the introduction of the KM matrix. The violation was discovered by observing the decays of neutral kaons. These particles offer a unique "window" through which to look for small CP violating effects. We discuss this next.

12.14 *CP* Violation: The Neutral Kaon System

The observations of neutral kaons have led to several fundamental discoveries in particle physics. K^0 and $\overline{K}^0$, with definite I_3 and Y, are the states produced by strong interactions (see Chapter 2). For example,

$$\pi^- p \to K^0\Lambda,$$
$$\pi^+ p \to \overline{K}^0 K^+ p.$$

However, experimentally it is found that K^0 decay occurs with two different

lifetimes:

$$\tau(K_S^0 \to 2\pi) = 0.9 \times 10^{-10} \text{ sec}$$
$$\tau(K_L^0 \to 3\pi) = 0.5 \times 10^{-7} \text{ sec.} \qquad (12.128)$$

In other words, the K^0 produced by the strong interactions seems to be two different particles (K_S^0 and K_L^0) when we study its weak decays. The same dilemma appears for the $\overline{K}^0$, and it was therefore proposed that the K^0 and $\overline{K}^0$ are nothing but two different admixtures of the K_S^0 and K_L^0, the particles associated with the short- and long-lived 2π and 3π decay modes.

In the absence of orbital angular momentum, the 2π and 3π final states differ in parity, with $P = +1$ and -1, respectively. We mentioned that these observations were in fact instrumental in the discovery of parity violation in weak interactions in 1957. For some time, it was thought that weak interactions were at least invariant under the combined CP operation. We make the conventional choice of phase of $|K^0\rangle$ and $|\overline{K}^0\rangle$ such that

$$CP|K^0\rangle = |\overline{K}^0\rangle.$$

Since the final 2π and 3π states are eigenstates of CP with eigenvalues $+1$ and -1, respectively (see Exercise 12.26), it is tempting to identify the neutral kaon CP eigenstates with K_S^0 and K_L^0:

$$|K_S^0\rangle = \sqrt{\tfrac{1}{2}}\left(|K^0\rangle + |\overline{K}^0\rangle\right) \qquad [CP = +1]$$
$$|K_L^0\rangle = \sqrt{\tfrac{1}{2}}\left(|K^0\rangle - |\overline{K}^0\rangle\right) \qquad [CP = -1]. \qquad (12.129)$$

To a very good approximation, this is true. However, in 1964 it was demonstrated that $K_L^0 \to \pi^+\pi^-$ with a branching ratio of order 10^{-3}. Therefore, a small CP violating effect is indeed present. An excellent summary of the experiments and other K^0 phenomena is given, for example, by Perkins (1982).

EXERCISE 12.25 Show that $C = -1$ for a photon and hence that $C = +1$ for a π^0.

Hint Under $e \to -e$, the amplitude corresponding to Fig. 1.9a will change sign.

EXERCISE 12.26 Show that in the absence of angular momentum, a $\pi^+\pi^-$ or $\pi^0\pi^0$ state is an eigenstate of CP with eigenvalue $+1$. Further, show that by adding an S wave π^0, we obtain CP eigenstates $\pi^+\pi^-\pi^0$ or $3\pi^0$ with eigenvalue -1.

Hint A $\pi^+\pi^-$ state is totally symmetric under the interchange of the π-mesons, by Bose statistics. Interchange of the particles corresponds to the operation C followed by P.

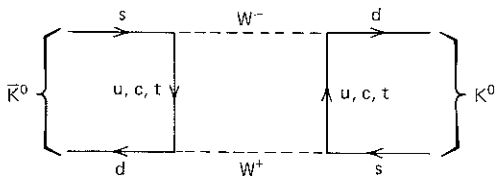

Fig. 12.21 Diagram responsible for $K^0 \leftrightarrow \overline{K}^0$ mixing.

The appearance of complex elements U_{ij} in the KM matrix may be related to the $\Delta S = 2$ transition mixing the $S = \pm 1$ K^0 and $\overline{K}^0$ states. The connection is not simple; the diagram of Fig. 12.21 is responsible for K^0–$\overline{K}^0$ mixing. With only u and c quarks exchanged (in the four-quark theory), the mixing would conserve *CP* and the resulting mass matrix would have eigenstates, (12.129), that differ by a small mass. In a six-quark theory, the values are slightly perturbed and $|K_S^0\rangle$ and $|K_L^0\rangle$ are no longer exactly *CP* eigenstates. Finally, it is widely believed that *CP* nonconservation in the early universe is the source of the apparent imbalance between matter and antimatter which we observe around us.